U.PORTO
FEUP FACULDADE DE ENGENHARIA
UNIVERSIDADE DO PORTO

U.PORTO
INSTITUTO DE CIÊNCIAS BIOMÉDICAS ABEL SALAZAR
UNIVERSIDADE DO PORTO

Exploring human placenta-derived hydrogels as a microenvironment for 3D cell culture

Ana Luísa Filipe Castro

Dissertation for the Degree of Master of Science in Bioengineering at Faculdade de Engenharia da Universidade do Porto and Instituto de Ciências Biomédicas Abel Salazar da Universidade do Porto

Exploring human placenta-derived hydrogels as a microenvironment for 3D cell culture

Ana Luísa Filipe Castro

Dissertation for the Degree of Master of Science in Bioengineering at Faculdade de Engenharia da Universidade do Porto and Instituto de Ciências Biomédicas Abel Salazar da Universidade do Porto

Supervisor: Cristina Barrias

Co-Supervisor: Aureliana Sousa

June 2018

“Start by doing what’s necessary;
Then do what’s possible;
And suddenly you are doing the impossible”

Saint Francis of Assisi

Page intentionally left in blank

Acknowledgments

First of all, I would like to thank my supervisor, Cristina Barrias, for the opportunity she gave me to be a part of this group and project during my dissertation. I am truly thankful for all the inspirational challenges she brought up during this past year, which allowed me to grow as a researcher. Cristina was always present, in every doubt and in every bad result, with a peaceful smile, transmitting all the motivation and optimism that a typical pessimist master student usually does not have.

I would also like to thank my co-supervisor, Filipa Sousa, for the exciting time we spent together in the last months. I am thankful for all the experience knowledge she gave me that allowed me to expand my abilities as a researcher and taught me to seek always for something bigger and better. Besides that, I am truthfully grateful for all the words, all the thoughts and all the effort to put away my pessimism, even though I deeply know that it was not an easy thing to do most of the days. And essentially thank you for all the memories we created in these past months, that surely will not be forgotten.

I would like to acknowledge Dra. Carla Ramalho, from Hospital São João, for the availability, which was crucial to the development of this project.

I would like to acknowledge Professor Ana Leite, Nilza Ribeiro and Gonçalo Soares, from Universidade Católica, for the cooperation and availability to let me use their facilities and equipment during the dissertation.

A special gratitude to Tália Figueiredo and Sara Neves for all the patience and support in different stages of this work, dedicating their own time to my concerns and experiments. To all my colleagues from both Bioengineered 3D microenvironments and Biocarrier groups, I cannot thank you enough for all the unbelievable moments that we lived in our laboratory, full of joy, dedication and cooperation that surely helped me throughout these months. I would like to highlight Pedro, to who I do not have words to describe how thankful I am for everything. More than a friend, you became this year an extraordinary lab partner, always being there, despite my good or (extremely) bad mood.

To my friends that were with me during this last five years, in every good and bad moments, with smiles and tears, without leaving my side even when times got tough. They say friends are the family we choose for ourselves, and if so, I am grateful for deserving a family like you and I hope we keep on making new memories for many years.

To my family, without whom all this journey would not even be possible to dream. To my parents and brother, for everything, for all the opportunities that I had throughout these 22 years, for all the moments, for all the care and love that you unconditionally gave me. What I am now, I owe that to you and to everything that you taught me during my childhood and youth. To my grandparents, which are, without a doubt, the most important foundation that my brother, my cousins and I have in our life. With every thought, every memory, every laugh and even every fight, they taught me how to see the important things in life and how to cherish them every day. I would like to thank specially to the one that, although not here present with me, is surely somewhere following me and, hopefully, proud of me. To you, grandma, today and forever, because my life will be yours until the day we meet again.

The research described in this thesis was financially supported by:

NORTE-01-0145-FEDER-000012 funded by North Portugal Regional Operational Program (NORTE2020) under PORTUGAL2020 Partnership Agreement through Regional Development Fund (FEDER).

Abstract

Organ and tissue decellularization has been widely explored as a strategy to produce extracellular matrix (ECM) biologic scaffolds for tissue engineering. Currently, different types of decellularized tissues/organs are being applied as scaffolds, both in *in vitro* cell culture studies and in different clinical applications for tissue repair.

Human placentas are widely available, can be harvested without harm to the donor and are commonly discarded as biological waste after delivery. Moreover, placental tissue contains abundant amounts of ECM components and important growth factors, thus providing a very appealing source for tissue decellularization. Through various treatments, effective ECM decellularization can be accomplished, but the original composition and structure might be affected to some extent. These effects are highly dependent on the decellularization agents used, and can be attenuated by optimizing protocols to each specific organ or tissue.

In this context, the aim of this work was the development and characterization of placenta-derived hydrogels, using optimized protocols for tissue decellularization and solubilization, and their evaluation as 3D matrices for in vitro culture of stromal cells.

Placental maternal villous samples were successfully decellularized following a 5-days protocol with SDS and DNAse treatments, adapted from a previous work. Histological analyses of decellularized tissue showed high removal of cellular/nuclear contents and adequate preservation of ECM components. Decellularized ECM (dECM) was solubilized through acid-pepsin digestion. In some samples, sterilization using supercritical CO_2 was also tested. This methodology allowed the successful production of hydrogels. These were characterized in terms of gelation kinetics and viscoelastic properties, which varied with the concentration of dECM and the sterilization. Biochemical analysis showed the presence of high amounts of total protein and glycosaminoglycans. Fibroblasts and mesenchymal stem cells (MSC) were cultured on-top of dECM hydrogel discs for 7 days, and cell viability, metabolic activity and morphology were assessed at different time points. Overall, although results showed some inconsistences, dECM hydrogels appear to provide favourable microenvironments for cell culture, supporting cell adhesion, viability and proliferation.

Taken together, these results show that protocols for decellularization/solubilization of placental maternal villous were successfully established, allowing the formation of hydrogels that show promise as human-derived matrices for cell culture. In the future it will be important to repeat and validate these experiments, specially using placentas from different donors to minimize tissue variability, which will be key for the future application of these materials.

Page intentionally left in blank

List of Contents

Abbreviation List

3D – Three dimensional

BCA – Bicinchoninic acid

BSA – Bovine serum albumin

CHAPS – 3-[(3-cholamidopropyl)dimethylammonio]-1-propanesulfonate

DAPI – 4',6-diamidino-2-phenylindole

dECM – Decellularized extracellular matrix

DMEM – Dermal fibroblast culture medium

DMMB – Dimethylmethylene blue

DNA – Deoxyribonucleic acid

ECM – Extracellular matrix

EDTA – Ethylenediamine tetraacetic acid

EGTA – Ethyleneglycol tetraacetic acid

EHS – Engelbreth-Holm-Swarm

FBS – Fetal bovine serum

GAG – Glycosaminoglycans

H&E – Hematoxylin and eosin

HA – Hyaluronic acid

HBSS – Hank's balanced salt solution

MSC – Mesenchymal stem cells

MT – Masson's Trichrome

ON – Overnight

PAA – Peracetic acid

PBS – Phosphate-buffered saline

PFA – Paraformaldehyde

RNA – Ribonucleic acid

RPM – Rotations per minute

RT – Room temperature

SDS – Sodium dodecyl sulfate

TBP – Tri(*n*-butyl)phosphate

List of Figures

List of Tables

Page intentionally left in blank

Introduction

1. Extracellular Matrix

The extracellular matrix (ECM) is a non-cellular component present in all tissues and organs, secreted and remodelled by cells. It plays a crucial role in the cellular microenvironment, providing structural and physical support for cells to attach, migrate and grow, and also acts as a reservoir of biochemical components that mediate cellular activities. [1], [2] In concert with soluble signals, ECM cues coordinate processes like differentiation, proliferation, survival and migration of cells, among others. Through matrix-bond growth factors and interaction with receptors, the ECM directly regulates signal transduction and gene transcription. [1] Although its basic composition is fundamentally water, proteins and polysaccharides, the characteristics of the ECM vary from tissue to tissue. [3] During development, biochemical and biophysical cues dictate tissue-dependent ECM specificities. [2] Besides that, its structure and composition are highly dynamic, as it undergoes constant remodelling, and can also be significantly altered under pathological contexts. The final characteristics of ECM dictate the biochemical and mechanical properties of each tissue and organ. [1]–[3]

The major components of ECM are structural proteins, including collagens and elastin, more specialized proteins like laminins and fibronectin, and glycosaminoglycans (GAG) in free (hyaluronic acid) or protein-conjugated (proteoglycans and glycoproteins) forms. The collagenous proteins can be divided into fibril (type I, II and III, for example) or network (type IV, for example) forming collagens and are responsible for tissue architecture, shape and organization, providing tensile strength. [2], [4] Laminins are often linked to type IV collagen networks and are crucial in embryonic development and organogenesis. [5] Fibronectin, secreted as dimers, has several important binding sites, namely to collagen, heparin and cell surface integrin receptors, and plays an important role in the attachment and migration of cells, among other cellular activities. [2] The negatively charged GAG lead to the sequestering of water and divalent cations, providing space-filling and lubrication functions to the ECM. Proteoglycans have a core protein to which GAG side chains are attached to. They have a wide range of molecular diversity, which results in a great variety of biological functions, such as elasticity, resistance to pressure and also cell signalling, through interactions with growth factors and their receptors, participating in important biological processes. [2], [4] Figure 1 shows a schematic drawing of ECM organization, with its major components. [6]

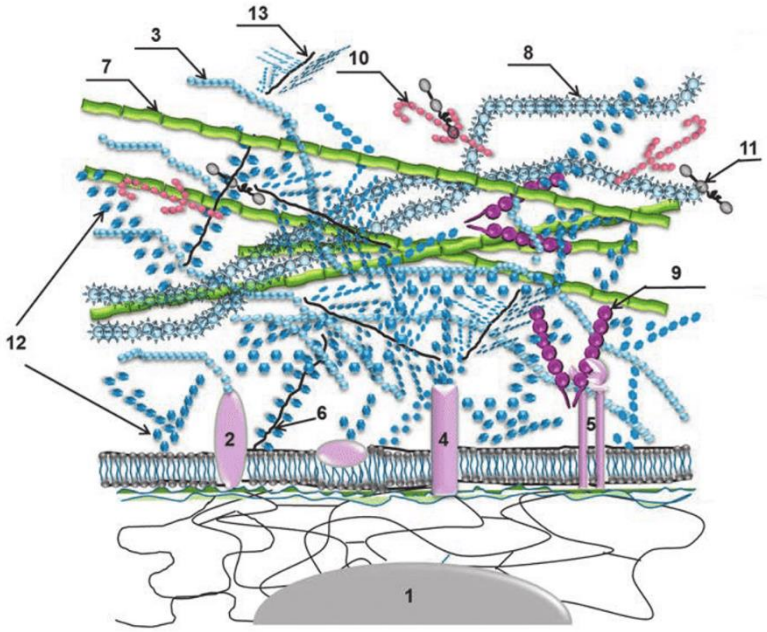

Figure 1 – Extracellular Matrix schematic organization. 1: Nucleus; 2: Hyaladherin; 3: Hyaluronic acid (HA); 4: Glycoprotein; 5: Integrin; 6: Syndecan; 7: Elastane; 8: Collagen; 9: Fibronectin; 10: Laminin; 11: Nidogen; 12: Gel-forming polysaccharides; 13: Small soluble proteoglycan. Adapted from [7]

1.1. ECM inspired materials

Although the human body has the ability to regenerate, this process only occurs in some tissues/organs, and in small defects. If there is a large defect or a severe injurie, healing is compromised or, in the worst case, does not occur. To overcome these situations, research has been focused on developing regenerative strategies in order to replace and regenerate the damaged tissues or to induce the body's self-healing capacity. These strategies often include the seeding of specific cell types in three-dimensional (3D) scaffolds, to recreate the natural 3D environment where cells reside in native tissues, the ECM, and their posterior implantation into patients. [8], [9]

Scaffolding biomaterials should ideally mimic the properties of the natural ECM. However, recreating the structural and functional properties of a specific tissue is a challenging task. [10] Different types of biomaterials can be used to produce ECM-like 3D scaffolds. Among those, hydrogels emerged as attractive candidates due to their inherent ability to closely mimic key features of the native ECM. Hydrogels are 3D networks that can often be formed under cytocompatible conditions, making them ideal for cell entrapment. In addition, they exhibit high water content and permeability, promoting efficient exchange of nutrients, oxygen and metabolites with the extracellular milieu. Being compliant structures, hydrogel-based matrices provide cells with adequate mechanical microenvironments, whose properties can be tuned to match

those of a variety of native tissues.[11] Both natural and synthetic hydrogels can be used, depending on the desired characteristics, namely in terms of mechanical support, biocompatibility and stability, among others. [12]. Currently available hydrogels can be broadly divided into two categories, according to the type of interactions they can establish with cells, namely bioactive and bioinert hydrogels. Bioactive hydrogels comprise those whose building blocks naturally possess direct (e.g. integrin-binding) and/or indirect (e.g. enzyme-susceptible domains) cell-interactive cues, being inherently cell instructive and/or responsive. On their turn, bioinert hydrogels comprise the ones that lack any type of cell-interactive domains. Both types of hydrogels can be chemically modified for inclusion of additional/new bioactive domains. [12] In both cases, these materials can be used as artificial ECMs and designed to recreate some of its functions and/or provide a 3D environment to cells. [13]

1.2. ECM derived biomaterials

ECM inspired biomaterials have shown great results, but also some weaknesses in what concerns biocompatibility and/or interaction with cells. Also, replicating the complex, and dynamic, nature of the ECM remains one major challenge in the design of ECM mimics. [14] In alternative, research has focused on ECM decellularization. One of the first reports on the use of decellularized tissue involved the culture of human keratinocytes and fibroblast on human decellularized skin, which was transplanted into a mouse model. [15] Several other works has been reported, using different types of decellularized ECM (dECM), from small intestinal submucosa [16], heart tissue [17], and esophagus [18], among others.

The principal aim of ECM decellularization processes is to remove all cellular components from a tissue or organ, namely to avoid strong immunological reactions upon implantation, but without compromising or damaging ECM components and structure. Different approaches have been used to achieve decellularization, some of which will be discussed herein. Once the process is completed, an ECM-derived 3D structure is obtained, with its composition varying depending on the method used and on the specific tissue/organ that was decellularized. Although the process might damage, to some extent, some structural tissue elements, such as elastic fibers or proteoglycans, one of the unique characteristics of decellularized ECM biomaterials is that they preserve specific biochemical/biophysical features of the tissue of interest. [12], [19]

Currently, different types of decellularized tissues are available in the market, with clinical success in several applications, such as burn wound healing and plastic

surgery, among others. However, there are also cases of failure, with host rejection to the tissue, due to immunogenicity of some dECM components. [20] The standardization of protocols is one of the main difficulties to overcome, since every tissue has its own ECM composition/structure. Therefore, the efficacy of a certain protocol varies with the type of tissue/organ. [12], [19]–[22] Another major challenge is to reduce donor-to-donor variability of dECM, which often requires pooling tissues from different donors.

2. Biomaterials from decellularized ECMs

As already pointed out, the intent of a tissue/organ decellularization process is to remove cellular components, while minimizing ECM disruption and maintaining its native biologic functions and physical proprieties. To achieve full decellularization, several approaches have been used, since parameters such as cell and/or ECM density and structural features depend on the type of tissue/organ. Decellularization processes may encompass different types of treatments: physical, enzymatic and chemical. Since each of them present advantages and disadvantages, and not all methods work efficiently in every case, a combination of approaches is generally used. An overview of the different decellularization methodologies, in terms of type of agent and technique (immersion vs. perfusion), is presented along the next sections.

2.1. Decellularization agents

2.1.1. Physical treatments

Physical treatments can be used to disrupt cell membranes, releasing cell contents and facilitating the removal of cells from the ECM. They can include agitation, sonication, mechanical pressure, freeze-thawing cycles or usage of supercritical fluids. All treatments are summarized in Table 1.

Mechanical agitation, using orbital shakers or magnetic stirring plates, as well as sonication are often used in combination with chemical procedures, to facilitate cell lysis and removal of cell debris. Protocols should be optimized, in terms of the speed of agitation, treatment length and volume of reagent, for each type of tissue, given its specific composition, density and volume. [23], [24]

In case of whole organs, the application of mechanical pressure gradients can be achieved through perfusion, for example. Perfusion (discussed in more detail on section 2.1.2.) can accelerate and improve the delivery of decellularization agents to the tissue, and may facilitate cell lysis, but it is not applicable in all cases. In fact, this

procedure showed efficacy, with minimal disruption to the 3D ECM architecture, only in tissues and organs that do not have a densely organized ECM (e.g. liver, lung, etc.). The application of pressure is reported to lead to a reduction in the exposure time to chemical agents during the experimental protocol. [23], [24].

Table 1. Examples of physical methods for decellularization of tissues/organs.

Physical Method	Mechanism of Action	Effects on ECM	Ref.
Mechanical agitation and sonication	Causes cell lysis. Facilitates chemical exposure and cell content removal	Aggressive agitation might lead to ECM disruption	[23]–[25]
Mechanical forces	Pressure can burst cells and by removing tissue, cells are removed	ECM can be damaged due to mechanical forces	[23], [24], [26]
Freeze-thawing cycles	Ice crystals disrupt cell membranes	ECM can be disrupted or fractured during rapid freezing	[23], [24], [27], [28]
Supercritical fluids	Critical fluids lead to cell removal	Minimal alteration in ECM mechanical properties	[24], [29]

Freeze-thawing cycles allow the formation of intracellular ice crystals that can disrupt cellular membrane, resulting in cell lysis. Temperature rates should be controlled in order to avoid ECM disruption, although some studies ([30], [31]) have stated that mechanical properties are not significantly alter during these cycles. Besides that, to minimize adverse effects, the use of cryo-protectants, such as trehalose, has been suggested. [32] Overall, these cycles can minimize the amount of chemical treatments needed afterwards. [24]

Extraction with supercritical fluids has recently been described as another alternative method to accomplish tissue decellularization, due to their low viscosity and high transport characteristics, allowing the establishment of simple and short protocols. It uses inert substances, like carbon dioxide that forms a critical fluid under a temperature of 32ºC and a pressure of 7.4 MPa (moderate conditions), to remove cells, while minimally altering ECM properties. At the end of the process, the decellularized tissue is already in a dry form, avoiding lyophilization steps that are often needed for long-term storage. The application of supercritical fluids for tissue decellularization remains largely unexplored, but it has been recently used in a number of studies, for example in aortic tissue, which was decellularized after 15 minutes. [24], [29]

All these procedures are usually combined with washing steps, however they are generally insufficient for complete decellularization of the tissue, and combination with other agents is typically needed. [12] [23]

2.1.2. Enzymatic treatments

Enzymatic treatments have been used in several tissues, due to their specificity for biologic substrates, and commonly employ proteases (trypsin, dispases), phospholipases, esterases and nucleases. The mechanism of action and effects of some of these enzymes are summarized in Table 2. [12], [24], [33]

Trypsin cleaves peptide bonds, with high specificity for cell adherent proteins, detaching cells from the tissue surface. This protein shows maximal activity at 37ºC and at pH=8. [23] However, prolonged treatment may have an adverse effect upon ECM components. For example, treatment with trypsin in pulmonary valve resulted in a disruption of ECM structures, reduction in protein content (as laminin and fibronectin) and GAGs content, as well as a decrease in tensile strength. [25] Despite that, the remaining ECM still supported endothelial cell growth. Overall, the exposure to trypsin should be keep to a minimum, to guarantee minimal disruptive effects on ECM structure and composition. [22], [31], [32]

Among dispases, dispase II is useful to separate epithelial cells from the substratum since it selectively cleaves fibronectin and collagen IV. This enzyme is mainly used in the first stages of decellularization, and requires combination with other decellularization agents. Dispases have also been typically combined with trypsin to improve cell removal in thicker tissues. [24], [34], [35]

Nucleases, as RNAse and DNAse, can catalyze hydrolysis of interior or terminal bounds in RNA and DNA (respectively), leading to their degradation. [23] However, residual cellular material may remain and some ECM components, such as fibronectin, can be reduced. [33] Phospholipase A2 is also used for hydrolization of phospholipids in the tissue, without damaging collagen structure and proteoglycans, but reducing GAGs content. [24], [33]

It is relevant to mention that proteases inhibitors may also play an important role in decellularization processes. On one hand, they are often used to protect ECM against proteases that might be released from disrupted cells. [24] The addition of aprotinin or leupeptin, for example, to the solutions in which the tissue is decellularized can provide such protection. On the other hand, the action of enzymatic agents can be hindered by natural inhibitors present in tissues, and the protocols should be planned to take this

into account. For example, decellularization studies using trypsin showed a decrease in its activity after 12h of treatment, due to natural protease inhibition. [36] Although enzymes provide removal of cell residues with high specificity, treatment with this agents alone is not enough to achieve complete cell removal. Therefore, they should be combined with other treatments for efficient decellularization.

Table 2. Examples of enzymatic methods for decellularization of tissues/organs.

Enzyme	Mechanism of Action	Effects on ECM	Ref.
Proteases	Cleaves peptide bonds, detaching cells from the substrate	Long incubation can reduce ECM components content and can disrupt ECM ultrastructure	[23], [33]
Nucleases	Catalyse the hydrolysis of bonds in RNA and DNA chains.	Not all content is removed. Can lead to immunogenicity.	[23], [24], [33], [37]
Phospholipases	Hydrolisation of phospholipids	Reduction in GAGs content	[33]

2.1.3. Chemical treatments

Chemical treatments can disrupt intercellular and extracellular bonds, which is important to allow sufficient exposure of cells to the chemical agents. The mechanism of action and effects of different types of chemical agents are summarized in Table 3.

Alkaline and acids treatments are often used to remove nucleic acids and solubilize the cytoplasm, by disrupting cell membranes and intracellular organelles. Acetic acid, peracetic acid (PAA), hydrochloric acid, sulfuric acid, sodium sulphide, calcium hydroxide are some examples of chemicals commonly used in decellularization protocols. [23], [38] Alkaline treatments have been used in decellularization of dense tissues, such, as dermis, but degradation/elimination of ECM components, such as collagens and growth factors have been reported. [34] Acids can dissociate DNA from the ECM but can also denature ECM proteins, reducing the construct strength, so there is the need to balance the doses and exposure time. [24], [36], [39], [40]

Non-ionic detergents have also been used to disrupt lipid-lipid and lipid-protein interactions, without damaging protein-protein interactions, leaving proteins in a functional conformation after treatment. [41] Triton X-100 is one of the mostly used non-ionic detergents, with times of exposure that can range from hours to weeks. [24], [42], [43] Depending on the tissue, this detergent showed different results. In the decellularization of a heart valve, for example, complete removal of nuclear material was achieved in the valvular structure, but not in the aortic wall. Regarding the ECM, a

loss of GAGs, laminin and fibronectin content was verified, as well as the formation of a less dense collagen network. [44], [45] Although efficient, Triton X-100 shows significant differences in its effects depending on tissues and on the other steps of the protocol, suggesting that adaptations of protocols should be done, taking into account the tissue density and cellularity. [23], [24]

Ionic detergents can also solubilize cell membranes, but they can disrupt protein-protein interactions, and may lead to denaturation of proteins. Sodium dodecyl sulfate (SDS) is the ionic detergent most commonly used. It shows a high efficiency in removing cellular components, with a better yield when compared to other detergents (such as sodium deoxycholate or Triton X-100, for example). [26], [43] In terms of ECM, SDS disrupts the native tissue structure and reduces the GAG content, but without removing collagen. To minimize these effects, SDS is ideally used in multiple washes with low concentrations of detergents for a short period of time. [46] Sodium deoxycholate is also efficient in removing cellular components, but has a more disrupted effect in the ECM, when compared to SDS. However, it has also been stated that SDS can be difficult to remove after treatment, possibly increasing cytotoxicity [23], [24], [34]. As with non-ionic detergents, the effect of ionic detergents varies with exposure time and with the organ or tissue under decellularization. [34], [47]–[49] Comparing SDS with Triton X-100, the first one appears to be more effective to achieve decellularization in dense tissues and organs, without affecting tissue mechanic characteristics.

Chemical treatments can also include zwitterionic detergents, which exhibit some of the properties of non-ionic and ionic detergents, having a higher tendency to denature proteins than non-ionic. 3-[(3-cholamidopropyl)dimethylammonio]-1-propanesulfonate (CHAPS), sulfobetaine-10 (SB-10) and sulfobetaine-16 (SB-16) are some examples of this type of detergents that have been used in decellularization protocols. [50]–[52] Protocols with CHAPS resulted in decellularized tissue with no difference in collagen content or histological features, but with impaired mechanical properties. However, this reduction is comparable to that obtained with Triton X-100 treatment. [23] CHAPS is most effective in thinner tissues and might be ineffective in thicker tissues, even when combined with SDS. [53], [54] SB-10 and SB-16 show better results in terms of ECM preservation, as well as better cell removal compared to non-ionic detergents. [24], [51]

Tri(*n*-butyl)phosphate (TBP) is an organic solvent that has been recently used as a chaotropic agent for decellularization, disrupting protein-protein interactions and removing nuclear remnants, but not completely. [42] The tensile strength of collagen

fibers and other biomechanical properties may be preserved, but a decrease in collagen content can be observed. [43] For dense tissues, decellularization using TBP appears to lead to better results than Triton X-100 and SDS, with a variation on the reported effects in terms of ECM constitution and properties. [21], [22], [32], [54]

Cycles with hypotonic and hypertonic solutions have also been used, which cause an osmotic shock and therefore result on cell lysis. [34] Ionic strength solution or deionized water are often used for this purpose, but they do not promote the removal of the cellular remnants resulting from cell lysis, needing an additional treatment. Minimal changes in ECM components and architecture are observed. [23], [50], [57]

Table 3. Chemical methods for decellularization of tissues/organs.

Chemical Method	Mechanism of Action	Effects on ECM	Ref.
Alkaline and Acids	Disruption of nucleic acids and solubilization of cytoplasm	Degradation of ECM structural components, as collagens, elimination of ECM growth factors and denaturation of ECM proteins	[23], [24], [34]
Non-ionic detergents	Disruption of lipid-lipid and lipid-protein interactions, without damaging protein-protein interactions	Loss of GAGs and laminin and fibronectin content	[23], [24], [41], [44], [45]
Ionic detergents	Solubilization of membranes, disrupting protein-protein interactions and fully denaturing proteins.	Disruption of the native tissue structure and reduction the GAG content without removing collagen.	[23], [24], [34]
Zwitterionic detergents	Similar to non-ionic detergents, but denaturing proteins.	Reduction in mechanical properties	[23], [24]
TBP	Disruption of protein-protein interactions	Loss of collagen, with minimal changes in mechanical properties	[23], [24], [34]
Hypotonic and Hypertonic Solutions	Osmotic shock to lyse cells	Cellular remnants not removed	[23], [34], [50]
Alcohols	Cell lysis	Alterations in collagen structure and tissue stiffness	[23], [24], [55]
Chelating agents	Disrupt cell adhesion	Used in combination with trypsin, only synergetic effects known	[23], [34]

Several types of alcohols, such as ethanol, isopropanol or methanol, may be used in decellularization protocols, with different consequences. For instance, they can lyse cells by replacing the intracellular water, and are often used as final wash in order to remove the residual nucleic acids from the tissue. [23], [24] They can also dissolve lipids due to their nonpolar nature, and there are studies showing that alcohols are more effective in removing lipids than lipases. [56]–[58]. Concerning the ECM, some studies showed alterations in collagen structure and tissue stiffness, when decellularization included ethanol or ethanol/acetone treatments. [55], [61]

Chelating agents as EDTA (typically used combined with trypsin) and EGTA can disrupt cell adhesions to the ECM and facilitate the removal of cellular material from the tissue, as a step during decellularization protocols. [23], [34]

2.2. Decellularization techniques: perfusion and immersion

Depending on the tissue/organ and final application, different decellularization technique can be adopted. Whole organ perfusion has been used in decellularization protocols that aim at preserving the 3D architecture and specific structures of the organ. Perfusion is done through the vasculature of the organ and it shows great efficiency in delivering the decellularization agents directly to cells and, inversely, in transporting cellular remnants out from the tissues. [24] As mentioned before, a pressure gradient can be applied during decellularization by perfusion, to obtain better results in terms of treatment length and preservation of ultrastructure. With a pressure gradient, decellularization agents are forced through dense tissues, allowing better cell removal from the ECM, while retaining collagens, laminin and GAGs. [34], [36], [59]

Different protocols have resulted in different 3D scaffolds with the geometry of native organs such as the heart, where the increase of pressure at which perfusion was performed showed to decrease the exposure time to the treatment, possibly due to a dilation of the vessels. [62], [63] Perfusion has also been used to decellularize lungs, showing that ECM major components and general structure could be maintained, allowing repopulation with cells. [53], [64]–[66] Liver and kidney have also been decellularized through perfusion, resulting in complete cell removal and maintenance of intact vasculature. [46], [67] In some studies, ECM analysis showed retention of laminin and collagen IV and capacity to support repopulation with specific tissue cells in both cases. [20], [68], [69]

However, perfusion systems require specific and expensive equipment, large quantities of solutions and can lead to an over-decellularization. In tissues whose vasculature is

not compatible with this technique, or is compromised, perfusion techniques may not be applied. [70] In some cases, maintaining the original 3D structure is not even a requisite. Under these circumstances, decellularization can be attained by chopping tissues into small fragments, to increase the area of contact, and immerse them in decellularization agents, under agitation for variable periods of time. This technique has been applied in different studies, using heart valves, spinal cord, cartilage, esophagus and dermis, among others. [39], [47], [71]–[76] Again, depending on the agitation speed and time, some ECM constituents can be lost or damaged, highlighting the need for optimizating each protocol depending on the tissue or organ characteristics.

Different studies with decellularized tissue/organs have been described, and Table 4 summarizes some of them.

The heart was the first organ to be successfully decellularized. Initially, the process was performed through perfusion of the aorta, with 1% SDS and 1% Triton X-100 treatment, with water washes between steps. [62], [77] Other protocols were tested afterwards, such as perfusion treatment with Trypsin and EDTA and with glycerol, NaN_3 and EDTA, for example. [63],[78] Similar treatments were adapted to immersion and agitation protocols, instead of perfusion techniques. [79]

Lung decellularization has also been performed, using rat organs. One of the first protocols to be published was based on 8 mM CHAPS protocol, while others used treatment with 0,1% SDS and Triton X-100, both using perfusion techniques. [53], [64] In fact, in this case, the decellularization time can be reduced using the trachea as a delivery method. [80]

Liver decellularization was first reported with a perfusion treatment combining SDS and Triton X-100, and followed by other protocols using trypsin/EDTA. Both used the tissue vascularization as a method for decellularization agents delivery and preserving its architecture and vascular network. [67], [80], [81]

Similar to what has been described with the liver, also kidney decellularization through perfusion has been studied and performed, preserving the vascular network of the organ. Most published protocols are based on SDS and Triton X-100 treatment, with the inclusion of a DNAse step in some cases. [20], [69], [77], [80]

Decellularization has been done in bone tissue (after demineralization), with enzymatic treatments in distilled water. [25], [82]. Also, decellularization of adipose tissue has been reported, for example, with isopropanol and SDS treatments. [79]

Table 4. Examples of decellularization protocols of various tissues/organs.

Organ/tissue	Technique	Solutions	Sterilization	Ref.
Kidney	Perfusion	0.5, 3, 6, 10% Triton X-100, 5 mM calcium chloride 5 mM magnesium sulfate 1M sodium chloride deionized water 0.0025% DNAse I	-	[69]
Lung	Perfusion	Heparinized PBS, 0.1%SDS, 1% Triton X-100, PBS	-	[64]
Liver	Perfusion	PBS, 1%, 2% and 3% Triton X-100, 0.1% SDS	-	[67]
Liver	Perfusion	0.02% trypsin/0.05% EGTA, Deionized water, PBS, 3% Triton X-100/0.05% EGTA	0.1% (v/v) peracetic acid 4% EtOH	[81]
Heart	Immersion	1%SDS, 1% Triton X-100, PBS	0.1% (v/v) peracetic acid 4% EtOH	[79]
Bone tissue	Immersion	0.05% trypsin/0.02% EDTA, PBS	-	[82]
Adipose tissue	Immersion	0.5% SDS, isopropanol, PBS	0.1% (v/v) peracetic acid 4% EtOH	[79]

2.3. Sterilization after decellularization

Prior to use decellularized tissues/organ *in vitro* or *in vivo* these need to be sterilized to eliminate eventual microbial agents that might lead to undesirable contamination, when in contact with cells, or immunological reaction upon implantation. Different treatments can be used, such as incubation in acids or solvents, ethylene oxide exposure or gamma and electron beam irradiation, but it is important to evaluate the additional effects of these processes on the tissues. [24], [34]

Treatment with PAA has already been reported as a means to disinfect decellularized materials. While this treatment can was shown to preserve ECM structure and function of several growth factors, it might show insufficient penetration into the tissue for a successful sterilization. [16], [24], [83]–[88]

Exposure to ethylene oxide can overcame the problem of tissue penetration, but on the other hand it may lead to significantly changes in ECM ultrastructure and properties. [89] Besides that, residues of ethylene oxide, classified as a being mutagenic and carcinogenic, can remain in the sample after treatment, potentially resulting in cytotoxicity and undesirable host responses. [90]

Gamma irradiation and electron beam irradiation often result in ECM degradation, mainly due to denaturation of key structural proteins. [91], [92]. The effect of low doses of these types of radiation is not well defined, with Crapo et al. stating that even with low doses the negative effects remain, and Keane et al. asserting that low dosages can increase the strength and modulus of the ECM scaffold. [24], [34] Lipid cytotoxicity and enzymatic degradation acceleration have been reported in processes with gamma irradiation, as well as a negative effects on the subsequent attachment of cells to the dECM. [91]

Supercritical carbon dioxide has recently been used in the process of sterilization, showing to decrease bacterial and viral contents, with minimal damage to ECM properties, when compared to the other processes, as seen for dermal dECM. It is compatible with biological materials, leaving no toxic residues in the material after treatment. [93] Amniotic membranes, lungs and bladder are some examples of decellularized tissues that have been sterilized with supercritical carbon dioxide. [89], [94], [95]

2.4. Hydrogels from decellularized ECM

As already discussed, preserving the native 3D architecture of tissues/organs is not relevant or even desirable for some applications, and the dECM can be further processed into different shapes including patches, sheets, microparticles and hydrogels. In the case of hydrogels, the ability to form them and the crosslinking kinetics is highly dependent on the biochemical profile of the tissue, namely on the remaining collagenous proteins after the decellularization process. [3]

There are two key procedures to achieve the formation of a hydrogel: initially, the ECM material is solubilized and then neutralized. Examples of conditions used for digesting decellularized tissues are presented in Table 5.

Tissue solubilization is often done via pepsin digestion. This enzyme acts through cleavage of non-helical telopeptide bonds of collagen structures, revealing the collagen fibril aggregates and has been used in the past decades to solubilize acid-insoluble collagen. [102]–[104] This digestion can be done following two different reported methods – “Freytes method”[97] and “Voytik-Harbin method”[105] – both relying on the use of an acid as a medium for pepsin digestion. Hydrochloric acid is used in the first method, while the second uses acetic acid, to achieve a pH in the optimal range for pepsin activity: 1.0-4.0. At pH 1.5 the enzyme shows 90% of maximum activity, at pH

Table 5. Examples of conditions used for digesting decellularized tissues.

Organ/tissue	Digestion Conditions	Gel Formation Conditions	Final ECM concentration	Ref.
Heart, cartilage, adipose tissue	0.5M acetic acid 10 mg pepsin to 100 mg ECM 48 h	pH adjustment 10M NaOH 37ºC	30 mg/mL	[79]
Liver	0.1M hydrochloric acid 10 mg pepsin to 100 mg ECM 48 h, RT	pH adjustment 0.5N NaOH 30' at 37ºC	10 and 20 mg/mL	[96]
Bladder	0.01M hydrochloric acid 10 mg pepsin to 100 mg ECM 48 h, RT	pH adjustment 0.1N NaOH 10xPBS 37ºC	10 mg/mL	[97]
Bone	0.01N hydrochloric acid 10 mg pepsin to 100 mg ECM 96 h	pH adjustment 1/10 0.1 N NaOH, 1/9 10xPBS 1 h at 37ºC	3 and 6 mg/mL	[82]
Brain and Spinal Cord	0.01N hydrochloric acid 10 mg pepsin to 100 mg ECM 48 h, RT	pH adjustment 0.1N NaOH 37ºC	10 mg/mL	[98]
Myocardium	0.1M hydrochloric acid 10 mg pepsin to 100 mg ECM 48 h	pH adjustment NaOH 2-4 h at 37ºC	6 mg/mL	[99]
Heart	0.5M acetic acid 10 mg pepsin to 100 mg ECM 48 h, RT	pH adjustment NaOH 10xPBS 37ºC	20 mg/mL	[100]
Umbilical Cord	0.01N hydrochloric acid 10 mg pepsin to 100 mg ECM 4h RT	pH adjustment 0.1N NaOH 10x PBS 45 min at 37ºC	8 mg/mL	[101]

4.5 it shows 35 % of maximum activity and at pH 7 or above it is irreversibly denatured. [106], [107] Regarding temperature conditions, at 25ºC pepsin has approximately 40% of activity, while at 37ºC it has above 90% of activity. [108] Although different times of ECM solubilization have been reported, varying from 48 to 96 hours, the solubilization should be considered as completed once there are no visible particles in suspension. [97] After the first step is finished, the solubilized ECM is neutralized to physiologic pH, forming a hydrogel when transferred to 37ºC. In practice, if not used immediately for

hydrogel formation, the solubilized and neutralized ECM should be kept at a low temperature, until further use at 37ºC, to assure a temperature-controlled gelation. [3]

2.5. Cell culture in decellularized ECM hydrogels

Native ECM represents the cell microenvironment, modelling cell behaviour, through physical and mechanical properties. Upon solubilization and hydrogel formation, the native 3D structure of the tissues is obviously lost, but important ECM characteristics and biologic activities are preserved, which make such hydrogels attractive matrices for 3D cell culture. [3], [98]

Different cell types, including cell lines, primary and stem cells have been used to test ECM hydrogels as 3D substrates for cell culture, which in many cases showed better outcomes than the traditionally used collagen type I hydrogels. For example, N1E-115 cell were cultured in brain dECM hydrogel, and neurite extensions were evaluated showing an increase in neurite length, possibly in response to the bioactivity of the scaffold. [98] In another study, hepatocyte cultured in a liver dECM hydrogel and aortic smooth muscle cells cultured in a dECM hydrogel showed better results in terms of cell viability. [97],[96] Moreover, calvarial cells cultured in bone dECM hydrogel, exhibited higher proliferation. [82]

Besides being used as matrices for 3D culture, dECM hydrogels can also be applied as surface coatings or gel layers for on-top cell culture. Matrigel™ is frequently used for these applications. Briefly, it consists on a solubilized basement membrane preparation, containing a mixture of insoluble proteins and growth factors secreted by Engelbreth-Holm-Swarm (EHS) mouse sarcoma cells. It has been widely used for culturing different cell types, particularly in vascular research for analysing the tubulogenic ability of endothelial cells, and in invasion assays, among others. However, its composition is not well defined, and the type and amount of proteins and growth factors may vary. [109] There is variability from lot-to-lot, which can lead to inconsistent experimental results and misreading conclusion, as it is impossible to discriminate the effect of a given component in cell behaviour. [110] Several studies comparing dECM hydrogels with commercially available ECM-derived Matrigel™ have been reported. For example, rat pre-adipocytes were cultured on the surface of adipose ECM hydrogels and formed bigger colonies when compared to the same conditions with Matrigel™, after 7 days of culture. [111] Thus, human-derived dECM hydrogels might provide an interesting alternative to Matrigel™, if pooled from different donors and produced under high quality standards to decrease compositional variability.

2. Decellularized placenta-derived biomaterials

3.1. Placenta: structural and biofunctional properties

The placenta is the fetal organ responsible for assuring the interchange of different substances between mother and fetus during pregnancy. This temporary organ provides to the fetus different functions that are performed, in adulthood, by several organs. It supports the nutritive, endocrine, respiratory and excretory functions and needs of the fetus during development, assuming a central role in this process. [112] [113]

Depending on the species, placentas show different characteristics, such as the method of uterine attachment, the number of tissue layers between the maternal and fetal circulations and the mechanism of substances transference. In humans, there are no layers separating the maternal blood from the fetal tissue. In other species, those components are separated, which translates to a significant difference in the molecules transferred between the mother and the fetus. All of this diversity results in a greater difficulty on the extrapolation of results from animal to human experiments. [114][115].
Besides the differences between species, within the same species, the collected placentas may exhibit some variability, depending on different factors, such as the intrinsic characteristics of the donor (age, health condition), the time and mode of delivery, the clamping of the umbilical cord and the collection method, among others. [116], [117]

3.1.1. Placenta Anatomy

A full-term human placenta has a diameter of about 22 cm, a central thickness of 2.5 cm, and an average weight of 470 g. The macroscopy anatomy of this organ can be divided into fetal or maternal surface, which will be briefly described herein. An additional section concerning the amniotic cavity membranes is also included. Figure 2 shows a schematic representation of placenta anatomy and vascular composition. [116], [118]

Fetal surface**.** The fetal surface is essentially represented by the chorionic plate, composed by the amnion and the chorion. The chorionic mesenchyme contains the chorionic vessels which continue into the vessels of the umbilical cord, inserted into the chorionic plate. The two umbilical arteries transport the fetal blood towards the placenta and divide into the chorionic arteries branch that supplies the villous trees, in the maternal surface. They further subdivide into thirdorder vessels terminal arterioles and, finally, capillary loops. It is within these loops that an optimal exchange between the

mother and fetus is accomplished, since there is a large endothelial surface area and connective tissue is nearly absent. [115], [116], [119], [120] The venus end of the capillaries return to the collecting venules, which form larger veins in the villous trees. These trees will drain to a large vein that becomes a chorionic vein since it perforates the chorionic plate. Finally, they continue into the umbilical vein and deliver the blood to the fetus. [115], [116]

Maternal surface. The maternal surface represents the basal of the placenta. It contains multiple cell types, including fetal extravillous trophoblasts and different maternal cells namely decidual stroma cells, natural killer cells, macrophages and other immune cells. [121] It also contains large amounts of ECM and is subdivided into 10–40 slightly elevated regions, the so-called lobes. These lobes show a good spatial correspondence with the position of the villous trees that arise from the chorionic plate. In terms of numbers, it is expected that in a full-term placenta, 60–70 villous trees arise from the chorionic plate, meaning that each maternal lobe is normally occupied by one to four lobules. [120], [122]

Membranes. The amniotic cavity is constituted by the amnion and the chorion, called together as ‘reflected membranes’. The amnion is continuous with the umbilical cord and composed by a single layered epithelium on a thin layer of avascular connective tissue – the amnionic mesenchyme. This avascular tissue is not completely fused to the chorionic mesenchyme, which allows to easily separate both tissues when processing the placenta. The chorionic membrane is composed of connective tissue and, at pregnancy term, it might also include remains of fetal blood vessels. [113], [116]

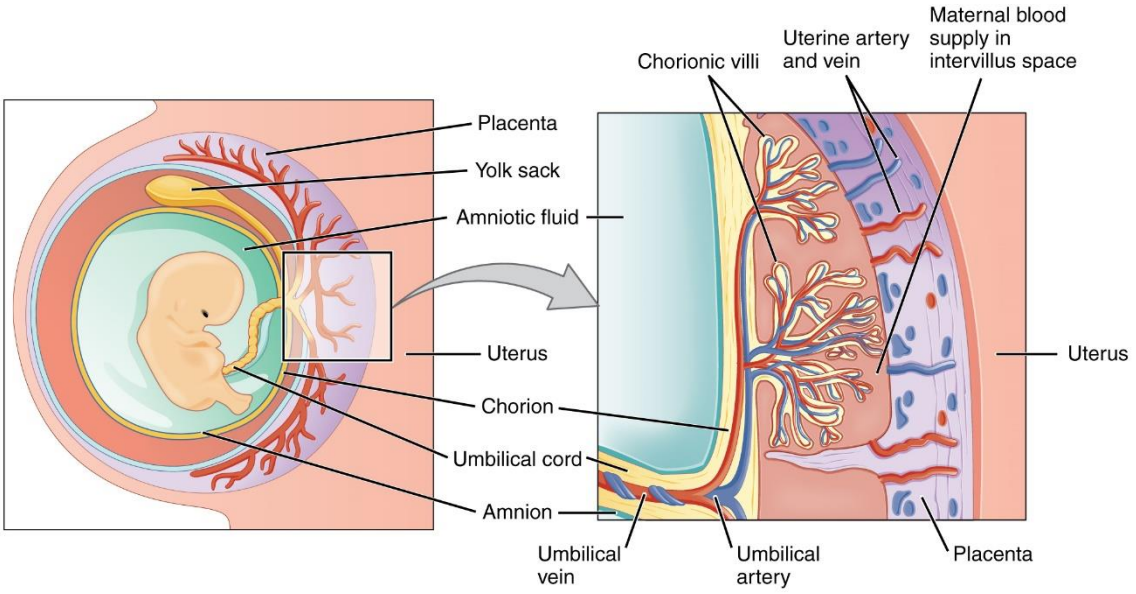

Figure 2 – Human placenta anatomy. Download for free at http://cnx.org/contents/14fb4ad7-39a1-4eee-ab6e-3ef2482e3e22@9.1

In a mature placenta, the intervillous space, although with highly branched villous trees, can accommodate approximately 350 mL of maternal blood.[123] The chorionic and the basal plates merge and form the smooth chorion, the fetal membranes and the chorion laeve, which is composed of three layers: the amnion, the chorion and the decidua capsularis. [116][120]

3.1.2 Placental extracellular matrix

The villous stroma of the placenta, among other functions, provides the environment for placental vascular development. [122] In the stroma of chorionic villi, the ECM, is mainly composed by collagens, laminins and fibronectin, as well as fibrillin I, thrombospondin I and tenascin C. [124][125]–[131] An analysis of ECM gene expression in human placenta showed genes of over 20 collagen chains, 50 non-collagenous glycoproteins and 20 proteoglycans. [124] Considering the collagen genes, both fibrilar (types I, II, III, V and XI) and non-fibrilar types (types IV, VI, VII, IX, XIV, XV, XVI, XVII, XVIII, XIX and XXI) are present. The distribution of ECM components in different locations changes along the pregnancy, such as, for example, collagen I and fibrillin I, representative of a major interstitial fibrillar species and a microfibrillar component, respectively. While some components exhibit a similar expression in both first trimester and term time points, others are more expressed on a term placenta than in the beginning of the pregnancy. For example, collagen I and IV are present in the stroma and vessels, both in first trimester and term placentas but, on the other hand, laminin and fibrilin, present in the stroma and vessels, are more expressed in the end of the pregnancy. [124], [125]

3.2. Decellularized placental tissues

Placentas are rich in ECM and other bioactive components, and are traditionally discarded as biological waste, thus providing a very appealing source for tissue decellularization. After delivery, they are among the most easily accessible human tissue Therefore, placental-based dECM biomaterials might have great potential in bioengineering applications and regenerative therapies [113], [132].

3.2.1. Decellularization placental protocols and applications

Some studies on the decellularization of amnion and chorion membranes, and of maternal villous have been described. The respective protocols will be briefly described below and are summarized in Table 6.

Table 6. Examples of protocols for placenta decellularization.

Placental tissue	Technique	Solutions	Ref.
Amnion	Immersion	0.5 M NaOH, 0.2%EDTA, 5% ammonium chloride, PBS	[133]
Amnion	Immersion	PBS, 10 mM Tris and 0.1% EDTA, 0.5% SDS, PBS	[134]
Maternal Villous	Immersion	distilled water, 0.5% SDS, DNAse and RNAse	[132]
Chorionic Plate	Immersion	distilled water, 2% N-lauryl sarcosine	[135]
Chorionic Vessels	Perfusion	hypertonic and hypotonic solutions, 1% Triton X-100 and 0.02% EDTA, DNAse	[136]

Different applications of decellularized placenta have been reported. For instance, amniotic membranes, native and decellularized, have been used for burn injuries treatment, where amniotic sheets are placed in the wounds [133], [137], [138], and also used for ophthalmologic treatments and postinfarct ventricular treatments [134], [139]. Similar to the amnion, the decellularized maternal villous has been used to develop ECM sheets to apply in skin treatments. [132]. In terms of chorionic components, decellularized chorionic vessels have been explored as small-diameter vascular grafts for endothelial cell culture, while decellularized chorionic plate has been digested in order to form a hydrogel where cardiomyocytes, adipose stem cells and endothelial cells were cultured. [135], [136]

Page intentionally left in blank

Materials and methods

1.1. Placenta tissue decellularization

Placentas were obtained from 4 women with normal pregnancies undergoing a term (38–40 weeks of gestation) scheduled cesarean section. Samples were obtained from Hospital São João, with informed consent from patients and after ethical approval from Ethics Committee for Health from the referred hospital. Placentas (figure 3 I) were processed within a maximum of 2 hours after delivery. Samples were immediately placed in PBS 1x (Phosphate-buffered saline, pH=7.4). The maternal villous region (figure 3 III) was separated from the chorionic plate (figure 3 II) and cut into fragments of around 1 cm^3. Membranes were also separated (figure 3 IV) and cut into sheets of around 5 cm^2. All material was stored at -80ºC until further use.

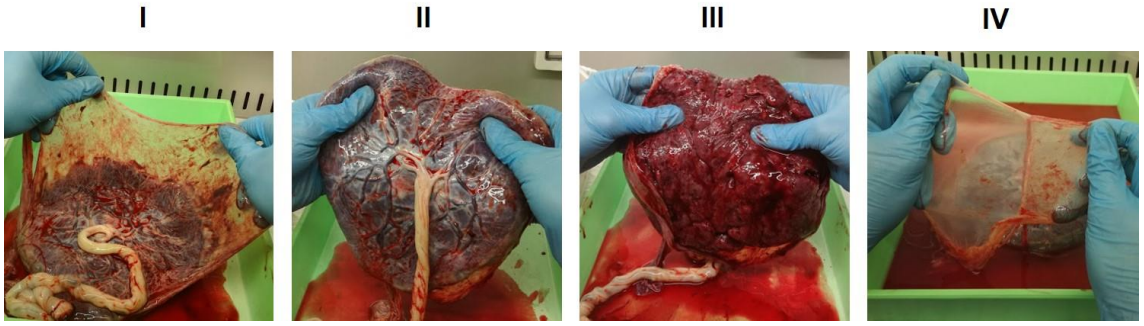

Figure 3 – Placenta dissection: I) Placenta after delivery; II) Chorionic plate and umbilical cord; III) Maternal villous; IV) Membranes separation.

Placenta decellularization was performed following a protocol adapted from Choi et al. [132] Samples were placed in spinner flasks (figure 4, I) and kept under magnetic agitation at 100 rpm (figure 4, III). First, several washes with distilled water with 0.01 wt.% NaN_3 (Acros Organic) were done to remove blood. The tissue was subsequently treated with 0.5% v/v SDS (Sigma-Aldrich) for 30 min, at room temperature (RT). To remove residual SDS, placenta samples were washed for 48 h with distilled water with 0.01 wt.% NaN_3.

Afterwards, samples were treated with 50U/mL DNAse (Panreac Applichem) in 10 mM Tris (VWR) and 2 mM $MgCl_2$ (pH=7.8), for 24 h at 37ºC, and then washed in distilled water with 0.01% NaN_3 during 24 h at RT. Control samples were treated only with distilled water with 0.01% NaN_3 during 5 days. All tissues were frozen, lyophilized and stored at -20ºC until further use.

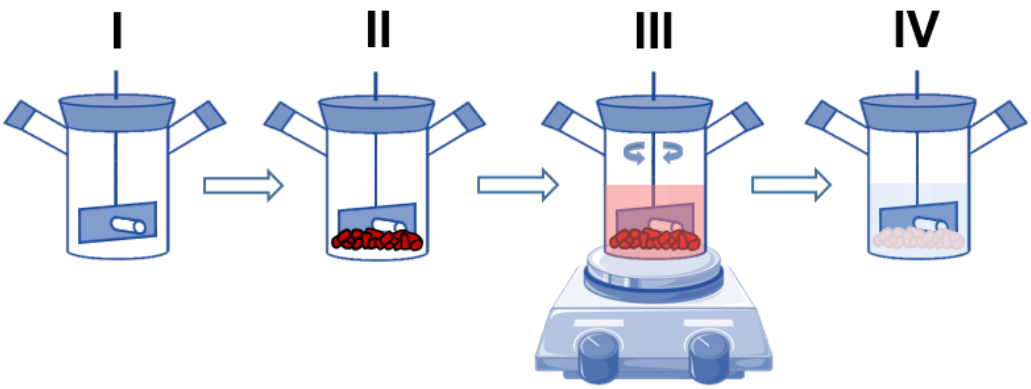

Figure 4 – Schematic representation of decellularization protocol: I) Spinner flask; II) Native maternal villous; III) Decellularization exemplification, with agitation; IV) Decellularized tissue.

1.2. Histological and immunohistochemical analysis

Native, control and decellularized tissues were fixed in 4% v/v paraformaldehyde (PFA) for 16 h and embedded in paraffin in an automatic rotational tissue processor (STP-120-1, MICROTOM). Tissue processing was set to graded series of 1 h each, starting by sequential immersion in ethanol (EtOH) solutions of increasing concentrations (70%, 90%, 98% and 100%), followed by immersion in ClearRite and finally immersion in preheated paraffin. Paraffin blocks were sectioned (3 µm) using a microtome (Leica RM2255). Paraffin-embedded sections were mounted on (3-aminopropyl)triethoxysilane (APES) coated glass slides, dried overnight (ON) at 37ºC and then kept at RT until use. All slides were deparaffinised in xylene and dehydrated using an ethanol gradient before stained.

Hematoxylin and Eosin (H&E) staining was used to evaluate the presence of nucleated cells and cellular components, while Masson's Trichrome (MT) staining was used to detect collagen fibbers. Images we obtained with a Zeiss Axioscop 2 microscope and processed using Fiji Imaging Software.

For immunohistochemistry, 10 mM citrate buffer (pH=6) and TE buffer (10 mM Tris, 1 mM EDTA, pH=9) were prepared. Slides were placed with the respective buffer (citrate buffer for fibronectin staining and TE buffer for collagen type-I and type-IV staining) in a water bath, at 90ºC for 20 min, and then washed in PBS for 20 min, extracted with 0.25% v/v Triton X-100 (Sigma-Aldrich) for 10 min under agitation and washed with PBS for 15 min. After, samples were blocked with 10% v/v fetal bovine serum (FBS) in PBS for 1 h at RT, and primary antibody solution with 5% FBS was added and incubated ON at 4ºC. Slides were treated with primary antibodies against fibronectin (1:200 dilution, F3648 Sigma-Aldrich) and human collagen type-I (1:100 dilution,

Rockland, reference 009-001-103)). Slides were then washed in PBS for 15 min, and incubated in secondary antibody solution (1:500 dilution) in 5% FBS (Alexa Fluor ® 488 goat anti rabbit, from Life Technologies; Alexa Fluor ® 594 goat anti rabbit, both from Life Technologies, respectively), for 1 h, at RT, protected from the light. In the end of the protocol, samples were mounted in vectashield with DAPI (for nuclear staining) medium (Vector Laboratories), and kept at 4ºC until analysis. Images were acquired using a confocal laser scanning microscope (Leica SP2 AOBS SE) and processed using Fiji Imaging Software.

1.3. Sterilization with supercritical CO_2

Lyophilized decellularized samples were sterilized using supercritical CO_2. The equipment (Parr Instruments series 4540 high pressure reactor, with 1200mL volume) is shown in figure 5A. Hydrogen peroxide (H_2O_2) was the solvent used in the process, which was performed at 140 bar, 40ºC, 600 rpm, for 6 h. The samples were sealed and then attached to the equipment using Teflon stripes, as depicted in figure 5B and 5C. *Bacillus pumilus* (Sigma) samples were also submitted to the process as a control group for the sterilization and cultured for 21 days in TrypticSoyBroth medium, at 37ºC, under aerobic conditions. Medium turbidity was assed to evaluate sterilization efficacy.

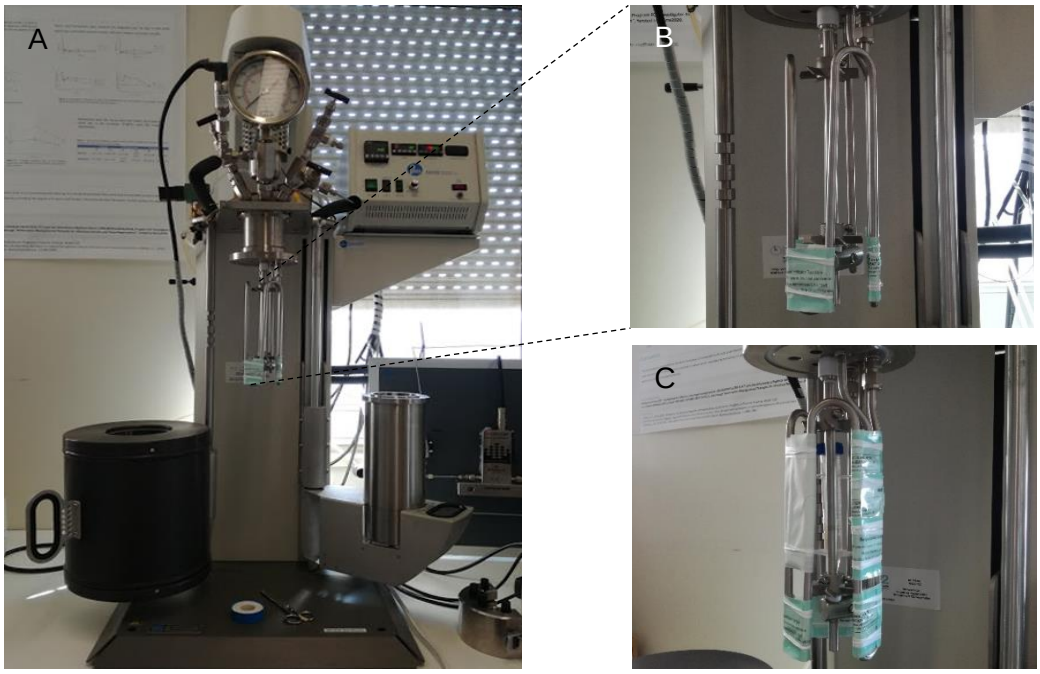

Figure 5 – Supercritical CO_2 sterilization. A: Sterilization equipment, before starting the process; B: Control samples attached to the equipment; C: All samples ready to be submitted to the process.

1.4. DNA quantification

DNA from native and decellularized tissues (control and test samples) was extracted and quantified using Maxwell ® 16 Tissue DNA Purification Kit (Promega), according to manufacturer's instructions. Briefly, 50 mg of tissue were placed in 200µL of Lysis Buffer and loaded into Maxwell ® 16 Instrument with 300µL elution buffer, following the Tissue DNA protocol. DNA content was measured on a spectrophotometer by absorption at 260nm (NanoDrop 1000, Thermo Fisher Scientific).

1.5. Solubilization of decellularized tissue

After being decellularized, lyophilized and/or sterilized, maternal tissue samples were minced into small pieces of around 5 mm^3. Tissue solubilization was performed through digestion with pepsin (Sigma) in 0.5 M acetic acid solution, at a ratio of 10 mg pepsin to 100 mg of ECM (dry weight), and a final ECM concentration of 40 mg/mL and 30 mg/mL. Samples were maintained under magnetic stirring, for 48 h at 37ºC.

1.6. dECM hydrogel formation

Solubilized samples were neutralized to pH 7.4 using 1M NaOH and 0.5M HCl and stored at 4ºC (pre-gel) until further use. With the pH adjustment, dECM concentrations diminished to 30 mg ECM/mL or 20 mg ECM/mL (from the initial 40 mg ECM/mL and 30 mg ECM/mL, respectively). Three different pre-gel solutions were obtained and used in the following tests: non-sterile 30 mg ECM per mL (3 wt.%), non-sterile 20 mg ECM per mL (2 wt.%) and sterile 30 mg ECM per mL (3 wt.%). To trigger gelation, pre-gel solutions were incubated at 37ºC for a minimum of 3 h. In order to form discs, 20 µL of pre-gel solution were placed between Teflon plates, with 1 mm spacers, and only then incubated for 3 h at 37ºC. For quantifications purposes, pre-gel was lyophilized a second time after neutralization and then reconstituted with water, at the desire concentration, based on the dry tissue weight.

1.7. Biochemical analyses of solubilized tissue

Total protein was quantified using the BCA Protein Assay kit (Pierce™, Thermo Scientific). The following samples were analysed: i) solubilized samples, consisting on pre-gel solutions of sterile, non-sterile and control tissue diluted to 2 mg/mL, and ii) reconstituted samples, consisting on lyophilized pre-gels (sterile, non sterile and control) reconstituted at a concentration of 2 mg dry tissue/mL. The protein content was

analysed following the manufacturer protocol. Briefly, a standard curve was generated using BSA, in a range concentrations from 0 mg/mL to 2 mg/mL. Samples and standards were incubated for 30 min at 37ºC with BCA working reagent and absorbance was measured at 570 nm in a microplate reader (Synergy™ Mx, BioTek).

Dimethylmethylene blue (DMMB) assay was used to measure the content of glycosaminoglycans (GAG) in the same solubilizes and reconstituted samples, also at 2 mg dry weight/mL. Following the manufacturer protocol, a standard curve was generated using chondroitin sulphate solution, in a range of concentrations from 0 µg/mL to 160 µg/mL. Samples and standards were incubated in DMMB reagent solution (40 mM NaCl, 40 mM glycine, 46 µM 1,9-bimethyl-methylene blue zinc chloride double salt, pH 3.0), and absorbance was read immediately after at 525 nm in a microplate reader (Synergy™ Mx, BioTek).

1.8. Rheological studies

Rheological properties of dECM hydrogels (non sterile ECM at 2 wt.% and 3 wt.%, sterile ECM at 3 wt.%) and Matrigel™ (Corning) were evaluated using a Kinexus Pro rheometer (Malvern Instruments, Malvern). The storage and loss modulus (G' and G'', respectively) of the different hydrogel formulations were recorded as a function of time and temperature, and their crossing point was defined as the gelation time [140]. The pre-gel solution (at 4ºC) was placed between 20 mm parallel plates with a 0.5 mm gap, at 37ºC for 14 h, at constant frequency (0.1 Hz) and strain (1%).

1.9. Cell culture

Human Dermal Neonatal Fibroblasts were purchased from ZenBio and mesenchymal stem cells were purchased from Lonza. Cells were thawed and maintained in culture at 37ºC in a humidified atmosphere with 5% v/v CO_2 in air, cultured in Dermal Fibroblast Culture Medium (DMEM, Invitrogen) with 10% v/v FBS, 1% v/v Penicillin/Streptomycin (P/S) and 1% v/v Amphotericin B or in DMEM with 10% FBS and 1% P/S, respectively. Cells were trypsinized when confluence was reached. For on-top culture, cells were seeded at a concentration of $1x10^4$ cells per disc (non sterile 3%, sterile 3% and Matrigel) in samples pre-incubated in culture medium to allow swelling. For 3D culture, cells were combined with pre-gel solution at a $1x10^7$ cells per mL, and the mixture was allowed to gelify for 2 h at 37ºC to allow gelification. In both cases, 500µL of the respective cell culture medium was added to each well and samples were incubated for different periods of time.

1.10. Viability assay

Viability was evaluated through Live/Dead Assay, using Ethidium homodimer-1 (Invitrogen) and Calcein-AM (Invitrogen) dissolved in DMEM without phenol red (2.5µL Ethidium and 2µL Calcein per mL of medium) and kept protected from light. The assay was performed at days 1, 3, and 7. Briefly, media was removed, samples were washed with DMEM without phenol red and then incubated in the Ethidium/Calcein solution for 45 min, at 37ºC. This solution was then replaced by DMEM without phenol red, and samples were imaged under a Zeiss inverted fluorescent microscope (Zeiss Axiovert 200, Carl Zeiss International). After acquisition, all images were processed using Fiji Imaging Software.

1.11. Metabolic activity

Metabolic activity was measured in all cell samples at days 1, 3, and 7. Briefly, a solution of 20% v/v resazurin (0.1 mg/mL; Sigma-Aldrich) in DMEM without phenol red was prepared and 400 µL were added to each sample. One well containing only resazurin solution was used as control. After an incubation of 4 h at 37ºC, fluorescence was excited at 530nm and read at 590nm, with a sensitivity of 70%, in a fluorimeter (Synergy Mx; Biotek).

1.12. Immunofluorescence imaging

At days 1, 3, and 7, immunocytochemistry was performed to evaluate cell culture in the hydrogel. Discs were washed in Hank's Balanced Salt Solution (HBSS; Alfagene) for 15 min, fixed in with 4% v/v PFA for 30 min, washed in HBSS for another 15 min and permeabilized with 0.1% v/v Triton X-100, in HBSS. Following, samples were incubated for 1 h in 1% BSA (Sigma Aldrich), washed in HBSS and incubated ON, at RT with agitation, with phalloidin (Alexa Fluor ® 488 Phalloidin; Invitrogen), diluted 1:40 in 1% BSA. Next day, discs were washed in HBSS, counterstained with DAPI for 10 min and washed again in HBSS. All samples were observed in confocal laser scanning microscope (Leica SP2 AOBS SE). After acquisition, all images were processed using Fiji Imaging Software.

1.13. Statistical analysis

Statistical analyses were performed using GraphPad Prism 7.04 software. For the quantification data and metabolic activity measurements, the non-parametric Mann–Whitney test was used. All tests were performed using a 95% confidence interval.

Page intentionally left in blank

Results and Discussion

1.1. Human Placenta Histology

After dissection, paraffin-embedded placental tissue was stained with H&E and MT to evaluate ECM abundance and distribution in different placenta components. Figure 6 shows both stainings in maternal villous, as well as a DAPI staining for nuclei identification. The maternal villous has a high nuclear content and is extremely irrigated, resulting in a large amount of blood accumulated within the tissue, as seen with detail in figure 6D. Vessels are surrounded by abundant collagenous ECM, as seen in figure 6B/E.

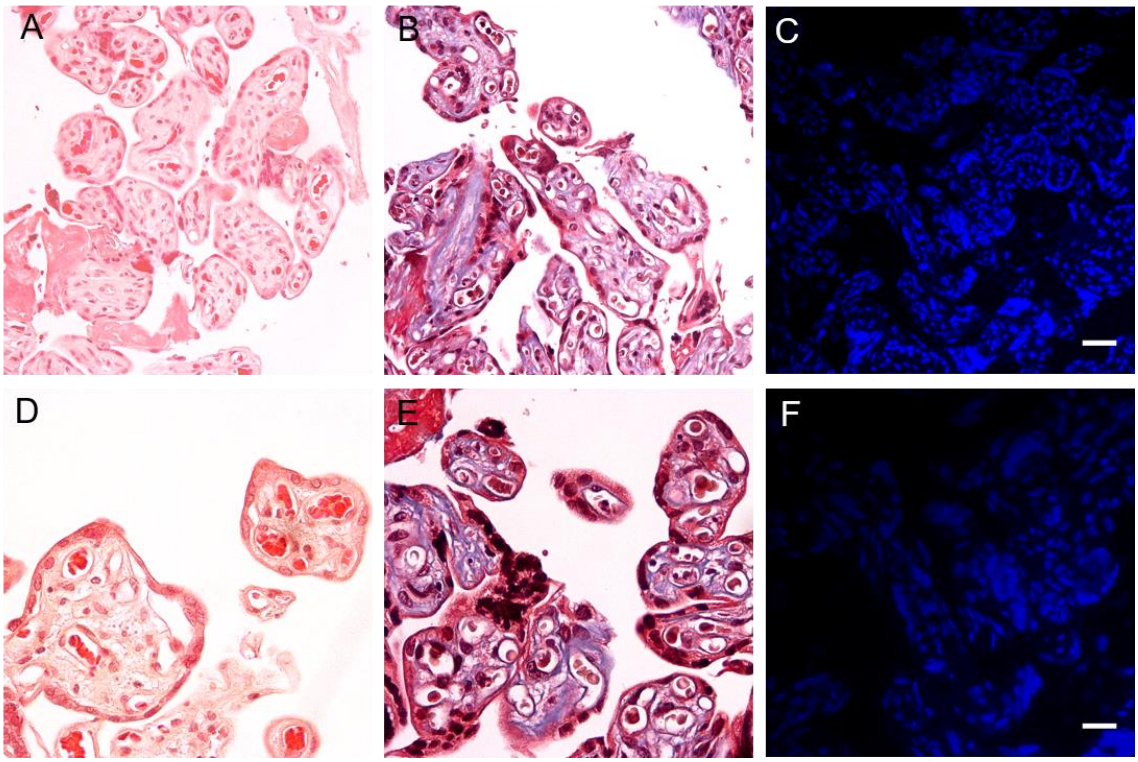

Figure 6 – Placenta maternal villous histology and nuclear content evaluation. A: H&E; B: MT; C: DAPI. Scale bar: 50 µm. D: Hematoxylin and Eosin; E: Masson's Trichrome; F: DAPI. Scale bar: 25 µm

Both amnion and chorion membranes are histological different from maternal villous, with a reduced cellular and ECM content. Amniotic membrane (figure 7 A/D) has a single layer of nucleated cells at the surface of the membrane and a connective tissue layer underneath, with presence of collagen, as seen in figure 7D. The chorion (figure 7 B/E) has a higher cellular content, being also richer in muscle fibres and collagen,

when compared to the amnion. Figure 7 C/F shows the amnion and chorion together, where it is possible to see that both membranes are fused, a phenomena that happens during early stages of embryonic development, and does not allow the establishment of a defined boundary between both membranes. [141]

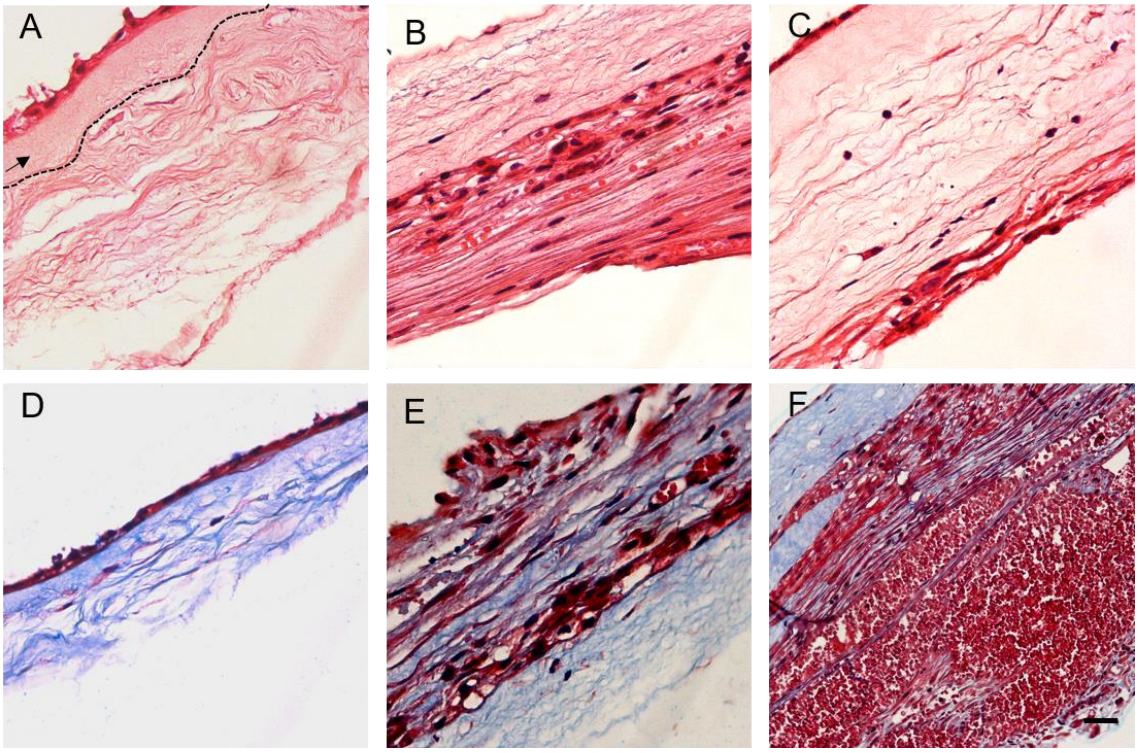

Figure 7 – Placenta membranes histology. A: H&E staining of amnion (arrow); B: H&E staining of chorion; C: H&E staining of amnion/chorion. D: MT staining of amnion; E: MT staining of chorion; F: MT staining of amnion/chorion. Scale bar 25 µm.

Considering that the main goal of this work was to achieve a hydrogel derived from decellularized placenta ECM, it was important to use a tissue rich in ECM proteins, namely collagen, as this would increase the chance of obtaining an hydrogel after solubilization [82], [142]. Comparing the different placental tissues analysed, the maternal villous was the one that better fulfilled this requisite. In addition to have a reduced content of ECM proteins, the use of each type of membrane, individually, could lead to some inconsistency between experiments. As mentioned, the separation between amnion and chorion is not well defined, and might differ from dissection to dissection, leading to some variability on the final composition of each membrane. Therefore, maternal villous was selected for subsequent decellularization.

1.2. Preparation of decellularized human placental maternal villous

Maternal villous tissue was fragmented into uniform pieces and decellularized following an optimization of a protocol reported in a previous work [132]. The original protocol consisted on an initial washing step in water to remove blood components, a SDS treatment followed by 4-days wash in water, and finally a DNAse/RNAse treatment (10 min, 37ºC) followed by 2-days wash in water. In the present work, an optimization is presented, where, after the initial washing step, tissue was submitted to a SDS treatment followed by 2-days wash in water, and a DNAse treatment (24 h, 37ºC) followed by 1-day wash in water. This way, the length of the decellularization protocol was reduced from 8 to 5 days. Another important alteration consisted on the use of spinner-flasks throughout the process, which presumable improved the efficacy of each step. A control group was also prepared, which was only submitted to water washing during the whole length of the protocol. Once the protocol was finished, tissue samples were frozen at -80ºC, lyophilized and stored at -20ºC. Figure 8 summarizes the key steps of the protocol, showing visual differences in the tissue samples along the five days treatment. A full detailed photographic report of all the decellularization steps is presented in Supplementary figure S1.

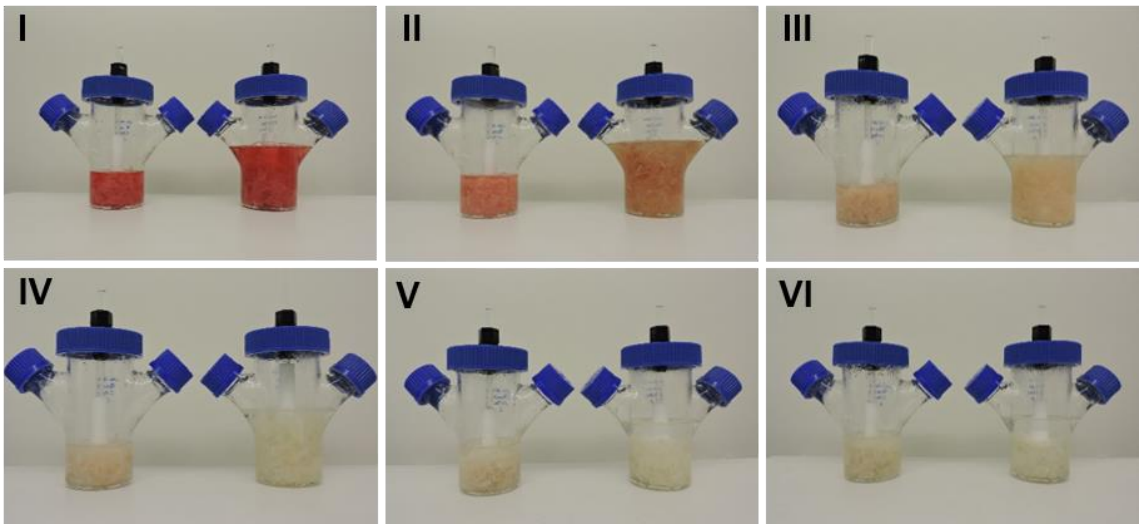

Figure 8 – Principal steps of decellularization protocol. I: Beginning of the protocol, with the tissue immersed in water; II: end of the first day; III: end of the second day; IV: end of the third day; V: onset of DNAse treatment; VI: end of the protocol. In all images, spinner flasks on the left represents control group.

The proposed protocol optimization was evaluated by comparing the decellularized samples from the 8-days original protocol (Supplementary figure S2A/B) and the 5-days protocol previously described (Supplementary figure S2C/D). The H&E and MT

staining of decellularized samples from both protocols, showed absence of cellular components and collagen maintenance after the processes are completed. This suggests that there are not any significant differences between protocols in terms of the final outcome, validating the optimization. Importantly, by the end of the 8-day protocol, tissue was already deteriorating, and some amount was being lost during solutions changes. This resulted in a lower yield of decellularized tissues, as compared to the original tissue. With the suggested protocol optimization, that disadvantage was overcome, avoiding the loss of material, while guarantying complete cell removal.

The DNAse / RNAse treatment suggested by Choi, J. S. et al., involved a 10 min exposure to the solution. When optimizing the protocol, based on the high cell content of present in native tissue (figure 6C/F), we decided to extend this treatment. Several DNAse exposure times have been reported in the literature, with different lengths, such as 4 h, 6 h, 16 h and 24 h [79], [143]–[147]. Here, to ensure total cell removal, the optimization protocol included a 24 h step of DNAse treatment. Some assays were run to test the effect of lower exposure times on nuclear components removal. Samples were taken from decellularized tissue at 0 h, 1 h and 3 h of DNAse treatment, and the remaining protocol was followed as described until completion. Samples were stained with DAPI and at all the three time points there were still nuclear components present in the tissue (Supplementary Figure S3). Although there was a significant reduction after 1 and 3 h, it did not lead to a complete nuclear removal, justifying a longer DNAse treatment.

1.3. Histological and immunohistochemical analysis of dECM

The effective removal of cellular and nuclear components from the tissue was confirmed by H&E and DAPI staining, while the preservation of ECM proteins was evaluated with MT, in control and decellularized samples. Results are shown in figure 9. Both control and decellularized samples showed the presence of collagen as seen in figure 9A. Although the control group exhibited less nuclear components than the native tissue (figure 6A/D), the control protocol was not sufficient to remove all the cells (figure 9A/C), as it would be expected. In contrast, SDS and DNAse treatments allowed full elimination of cellular components from the tissue, and significant reduction of nuclear materials, as seen with DAPI staining (figure 9F). However, the optimized protocol apparently did not significantly affect the structure and collagenous content of ECM, as suggested by the MT stainings in figure 6 B/E and figure 9 D.

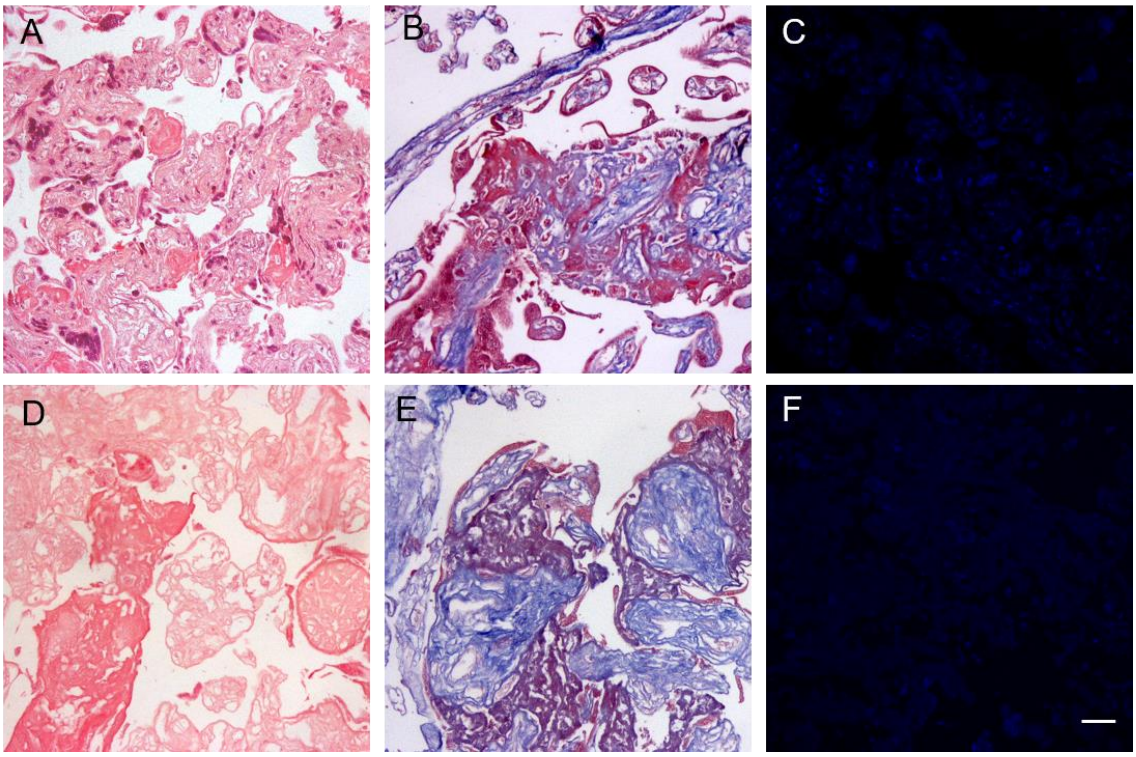

Figure 9 – Validation of decellularization protocol. A: H&E staining of control group; B: MT staining of control group; C: DAPI staining of control group; D- H&E staining of decellularized sample; E: MT staining of decellularized sample; F: DAPI staining of control group Scale bar: 50 µm.

Immunostainings for Fibronectin, Collagen type I and DAPI were also perfomed, for a better assessment of the differences between native, control and decellularized tissue, in terms of ECM changes in content and/or organization. A difference in fibronectin organization was observed between the native tissue and decellularized tissues submitted to both treatments (figure 10). This was somehow unexpected, since we found no reports stating that treatments similar to the ones used in the proposed protocol would damage fibronectin, contrary to enzymatic treatments with trypsin and dispase. [23] Nevertheless, the protein is still substantially present in the decellularized tissue, as seen in figure 10, suggesting that the apparent alteration might be more associated with structural features. This was not considered a major issue in the present work, given that the main goal was the posterior tissue solubilization for hydrogel formation.

On the other hand, the structure and content of collagen type I seemed to be well preserved (figure 11), both in control and decellularized tissue. This was expected, since previous studies reported that SDS might disrupt the native tissue structure but

without significantly removing collagen.[46] Decellularized samples exhibit a high abundance in collagenous tissue, as desired.

In both cases, the pattern of DAPI staining confirmed previous histological conclusions. The control group exhibited reduced nuclear content, as compared to native maternal villous, while the decellularized tissue was almost nuclei free, as seen in figure 10 and 11.

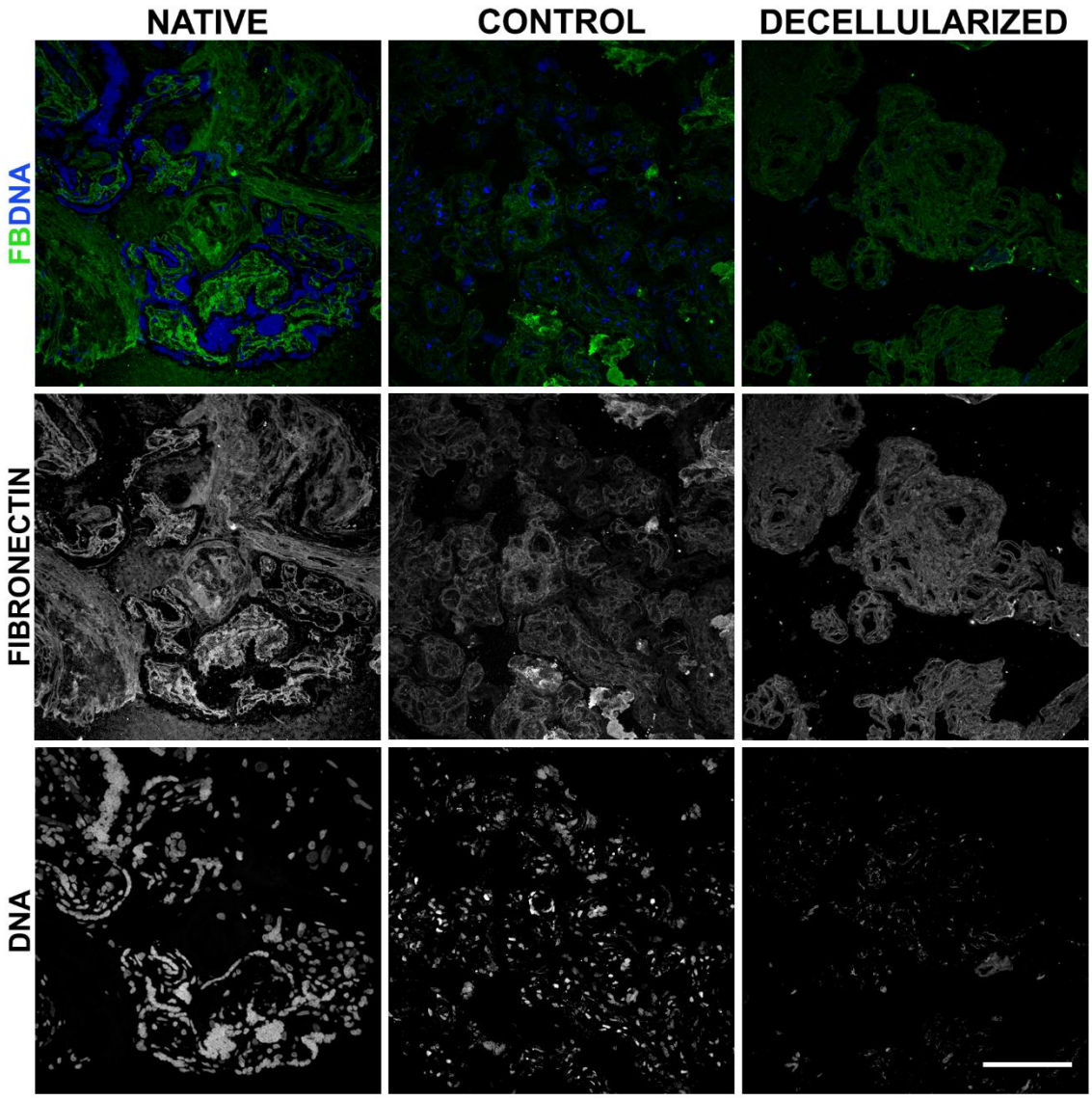

Figure 10 – Validation of decellularization protocol. Immunostaining for Fibronectin and DAPI staining in native, control and decellularized sample. Scale bar: 100 µm

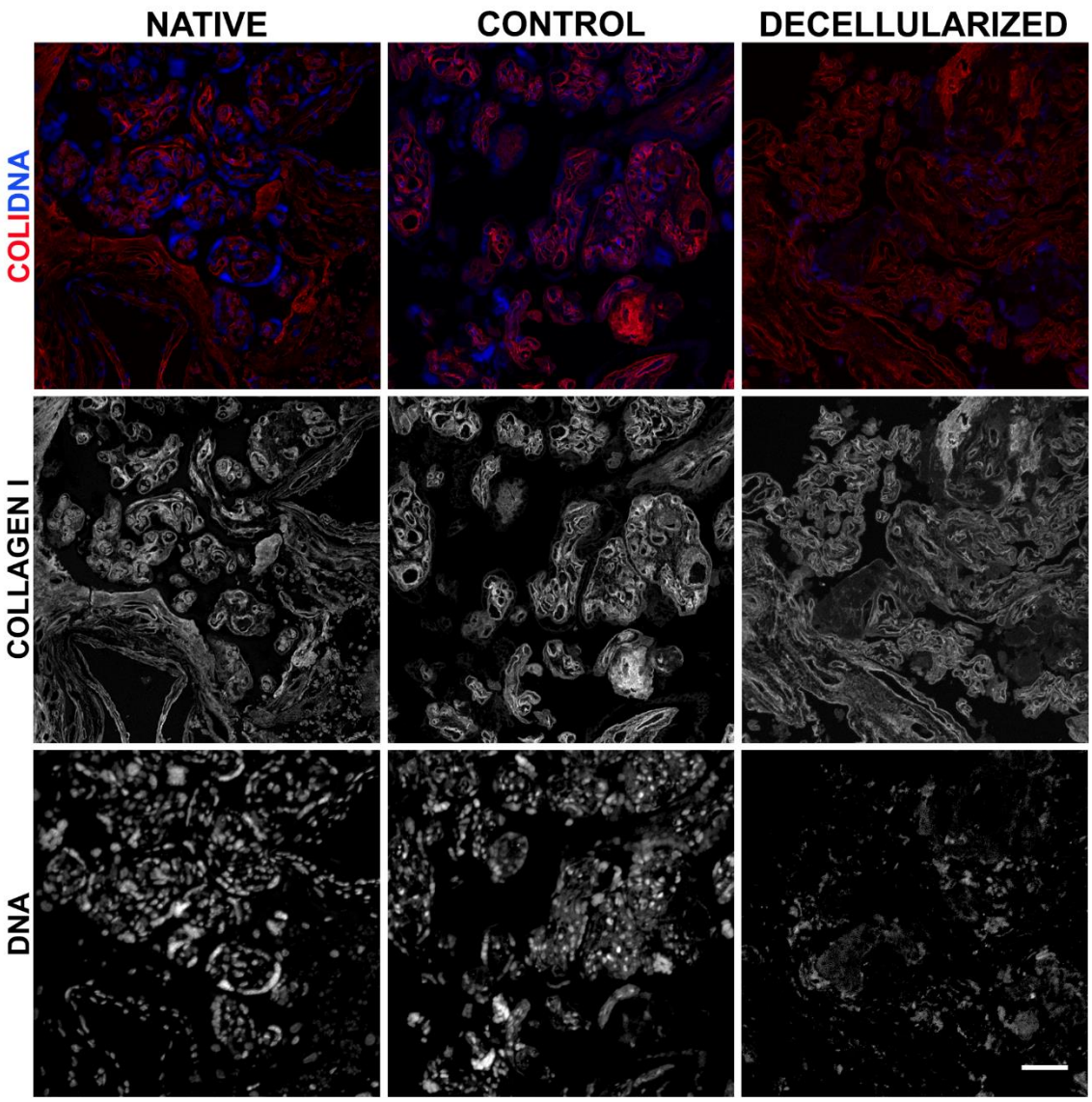

Figure 11 – Validation of decellularization protocol. Immunostaining for Collagen type-I and DAPI staining in native, control and decellularized sample. Scale bar: 100 µm

1.4. Placenta dECM sterilization

After lyophilization, samples were sterilized using supercritical CO_2, for 6 h. After treatment, samples remained dry. *Bacillus pumilus* were cultured for 21 days at 37ºC, under aerobic conditions. Medium turbidity was evaluated and results showed that those organisms did not survive to the sterilization and, therefore, ensured that placental tissue samples were sterilized. Biochemical and mechanical characteristics of the sterile sample will be evaluated further.

1.5. DNA quantification

DNA from native, control and decellularized tissue was quantified. As concluded before with histological and DAPI staining, an effective nuclear removal was only accomplished with the decellularization protocol. As depicted in figure 12, there was a slight reduction on DNA content from the native tissue (2749.48 ± 552.63 ng/mg tissue) to the control group (1064.71 ± 153.98 ng/mg tissue), which significantly decreased on decellularized samples (4.95 ± 3.62 ng/mg tissue, p value<0,05), resulting in a 99.9% reduction from native to decellularized tissue. Original 8-days protocol showed a smaller decrease in DNA content from native tissue (772.0 ± 224.04 ng/mg placenta) to decellularized tissue (34.3 ± 13.2 ng/mg placenta). [132] Comparing DNA quantification from both protocols, 5-days treatment resulted in a more efficient DNA tissue removal.

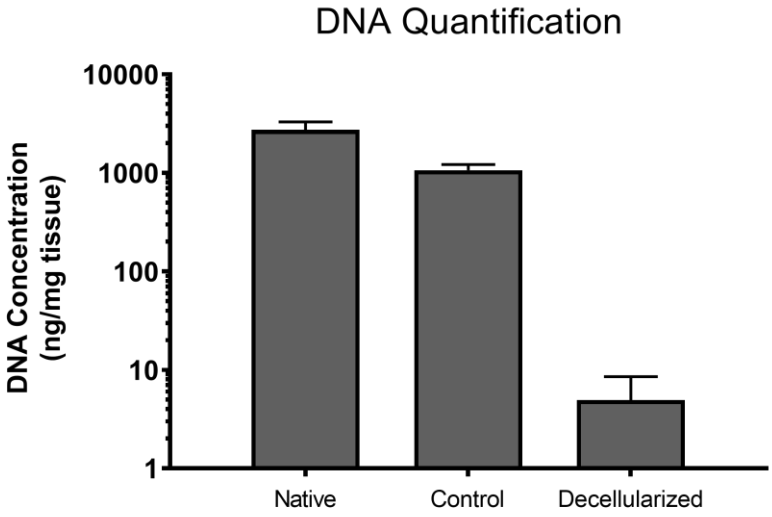

Figure 12 –DNA quantification in native, control and decellularized tissue (n=3).

1.6. Placenta dECM solubilization and gel formation

Lyophilized decellularized samples (sterile and non sterile) were solubilized through pepsin digestion in acetic acid, for 4h under magnetic agitation, at 37ºC at a concentration of 40 mg of dry ECM per mL of solution. In the end of the treatment, a viscous solution was obtained (figure 13A).

To inhibit the action of pepsin, pH was adjusted to 7.4, using NaOH and HCl (figure 13B). This adjustment increased the solution volume, consequently decreasing the final ECM concentration to 30 mg dry ECM/mL solution. To investigate the gel-forming ability of the solubilized ECM (pre-gel), a sample was taken, incubated ON at 37ºC and evaluated afterwards (figure 13C). The remaining pre-gel was kept at 4ºC until further use.

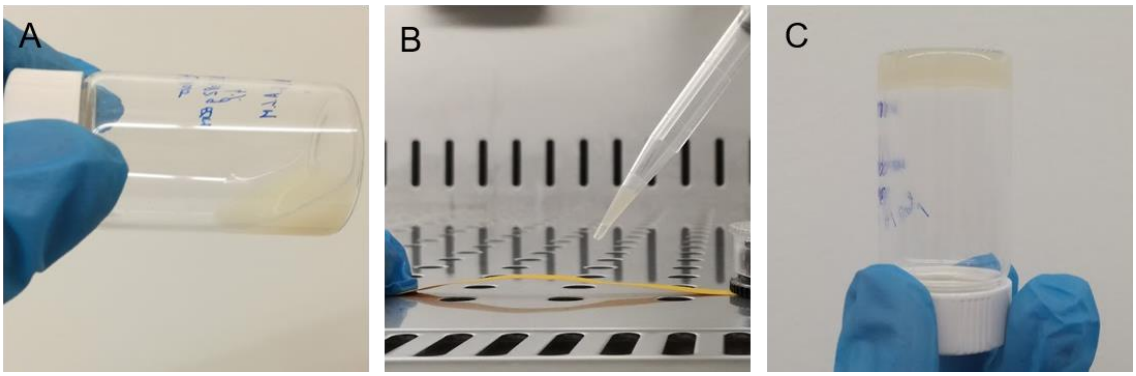

Figure 13 – Formation of placenta dECM hydrogel. A: Solution after solubilization; B: pH adjustment; C: Hydrogel formed after overnight incubation at 37ºC.

1.7. Biochemical characterization of solubilized dECM

Decellularized ECM was characterized in terms of total protein and GAGs content, in order to evaluate the effects of the proposed protocol and of the sterilization process on its major components. Two types of samples per condition (control, non sterile and sterile samples) were evaluated: pre-gel solubilized ECM and reconstituted ECM, (which after solubilization and neutralization was lyophilized, stored and finally reconstituted with water). All results are presented in figure 14.

1.7.1. Total protein quantification

Total protein was assed using BCA quantification kit. Results are shown in figure 14B. Concerning both types of samples, control group shows the lower concentration of protein per mg of dry ECM. While this was unexpected, it may eventually result from an artefact in the calculations. In fact, since control group is not fully decellularized, there are still cellular components left (as seen, for example, in section 1.5.) which contribute to the total mass of dried tissue that was originally weighted, solubilized, lyophilised and reconstituted for analysis. Therefore, when calculating the amount of protein per dry weight, we are in fact normalizing samples with respect to different things. This might possibly explain the apparently lower percentage of protein in the control tissue (0.36 ± 0.00 mg/mg dry ECM). An analogous conclusion can be taken when looking at results from non-sterile and sterile samples. During sterilization, other tissue components might have possibly been eluted, resulting in a higher concentration of proteins per mg of dry ECM (0.71 ± 0.08 mg/mg), as compared to non-sterile samples (0.49 ± 0.03 mg/mg).

Comparing solubilized and reconstituted samples, protein concentration in control samples showed no significant difference between both conditions (0.36 ± 0.00 vs 0.41 ± 0.05 mg/mg, solubilized and reconstituted, respectively). However, in sterile and non-

sterile conditions there were relevant changes in protein concentration. In non sterile samples, there was a significantly increase of protein concentration per mg of dry ECM after reconstitution (0.49 ± 0.03 vs 0.71 ± 0.05 mg/mg, p value<0.05, solubilized and reconstituted, respectively), while in sterile samples this protein concentration decreased after reconstitution (0.71 ± 0.09 vs 0.55 ± 0.02 mg/mg, solubilized and reconstituted, respectively). Such inconsistent differences between solubilized and reconstituted samples might again be related with the composition of the "dry tissue" that is weighted and used for normalization. In the case of the reconstituted samples, besides the dECM, the lyophilisation product also contains pepsin and salts from the digestion/solubilization process, which amount is difficult to control/quantify, that also contribute to the total weight.

1.7.2. GAGs quantification

GAGs content was measured in the same samples described above (figure 14C). Similar to what was described for the protein quantification, control samples exhibit the lower GAGs content, and no significant difference between solubilized and reconstituted samples (18.37 ± 1.26 vs 11.74 ± 4.69 µg/mg, respectively). Non-sterile samples show a significant reduction in GAGs content, when comparing solubilized to reconstituted samples (26.70 ± 0.52 vs 17.62 ± 3.72 µg/mg, pvalue<0.05 respectively), and the same for the sterile samples (30.51 ± 3.38 vs 24.27 ± 3.33 mg/mg, solubilized and reconstituted, respectively). A reduction in GAGs content as a consequence of the decellularization protocol was expected, since, as it was previously described, SDS treatment has been reported to damage GAGs, thus reduction their content. [46] Here, the reduced time of SDS treatment, and the several washes that followed it to completely remove all SDS, might have been contributed to the preservation of GAGs in the final samples. The inconsistencies found when comparing some of the conditions are likely to be related with the same issues described above for the protein content.

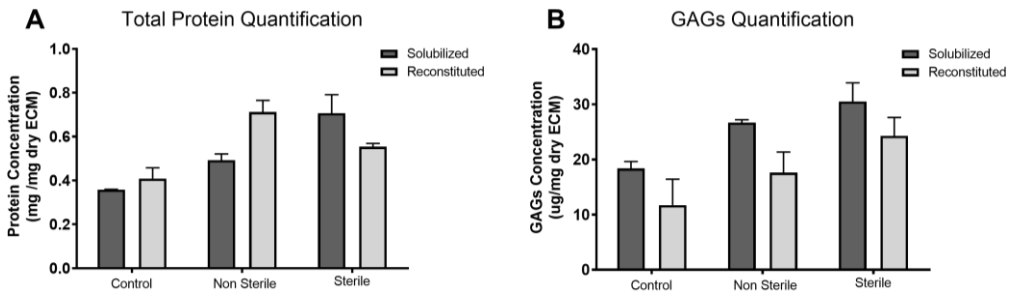

Figure 14 – Total protein (A) and GAGs (B) quantification in control, non-sterile and sterile samples (solubilized and reconstituted) (n=3)

In future studies, these issues should be taken into account, and a better way of normalizing results must be found. Nevertheless, taken together results from protein and GAG quantification suggest that the proposed protocols did not lead to a significant reduction of their contents, even after sterilization, which can be considered as a good outcome.

1.8. Rheological characterization

Rheological properties of neutralized dECM pre-gels were determined with a rheometer. Gelation kinetics was measured in three different types of samples: non-sterile (at 2 and 3 wt%) and sterile (at 3 wt%). Matrigel™ was used for comparison.

1.8.1. Gelation kinetics

To analyze the gelation kinetics of dECM hydrogels, pre-gel solutions (stored at 4ºC) were placed in the rheometer at 37ºC to induce gelation and submitted to a time sweep of nearly 14 h (1 h in the case of Matrigel™). Frequency and amplitude conditions were determined based on Matrigel™ linear-viscoelastic regime, stated in literature. [148] For all samples, in the end of the process, a thin disc (0.5 mm height, correspondent to the selected gap) was obtained, with a regular shape and uniform appearance. The crossover between storage and loss modulus (G' and G'', respectively) indicates the gelation time of the solution. Results of time sweep of analysis are shown in figure 15. The crossover for the 3 wt.% non-sterile hydrogel occurred almost immediately after the beginning of the assay (at t=5 min, G'= 3.62 ± 2.52 Pa and G''=2.73 ± 1.46 Pa). However, as seen in figure 15A, the parameters only stabilized after 2 to 3 h, at G'= 382.30 ± 80.68 Pa and G''=45.85 ± 8.39 Pa , remaining stable until the end of the test. The dECM hydrogel with lower concentration (2 wt.% non-sterile, figure 15B) was also formed almost immediately when at 37ºC (at t=5min, G'= 126.74 ± 89.49 Pa and G''=28.06 ± 20.00 Pa) reaching stability within approximately 2 h, at values of G'= 98.64 ± 16.06 Pa and G''=15.9 ± 1.99 Pa. The effect of sterilization was evaluated using sterile pre-gel at 3 wt.%. After t=5min, analogous to the other samples, the hydrogel was already formed, with G'= 5.17 ± 6.31 Pa and G''=3.82 ± 4.30 Pa, and G' and G'' stabilized after 1 to 2 h (53.85 ± 2.52 Pa and 6.44 ± 1.46 Pa, respectively). Matrigel™ gelation was evaluated along 1 h, based on literature studies that state that 30 min is enough to guarantee that the formed hydrogel reaches stable modulus values. In this test, the plate was previously set to 4ºC, to avoid Matrigel™ gelation before the beginning of the time sweep assay. In the first minutes recorded, temperature was still rising and it was under those conditions that hydrogel formation occurred. As seen in figure 15D, at t=2min and T=32ºC the recorded values were G'=

8.81 ± 3.53 Pa and G''=4.36 ± 0.82 Pa; and after 5 to 10 min both modulus had stabilized (G'= 73.95± 24.75 Pa and G''=7.77 ± 2.04 Pa).

Taken together, results show that while G' and G'' crossover occurs within a short time frame, solubilized dECM requires some additional time form a stable gel. These results were corroborated by another experiment (data not shown), where pre-gel solutions were placed in Teflon molds to form discs and left at 37ºC for 2h. After that time, while the pre-gel exhibited a more solid-like behaviour, hydrogel discs were not formed. However, when left overnight at 37ºC the same samples were able to form discs with sufficient integrity, indicating that a longer period of time is needed for the formation of a stable, solid hydrogel.

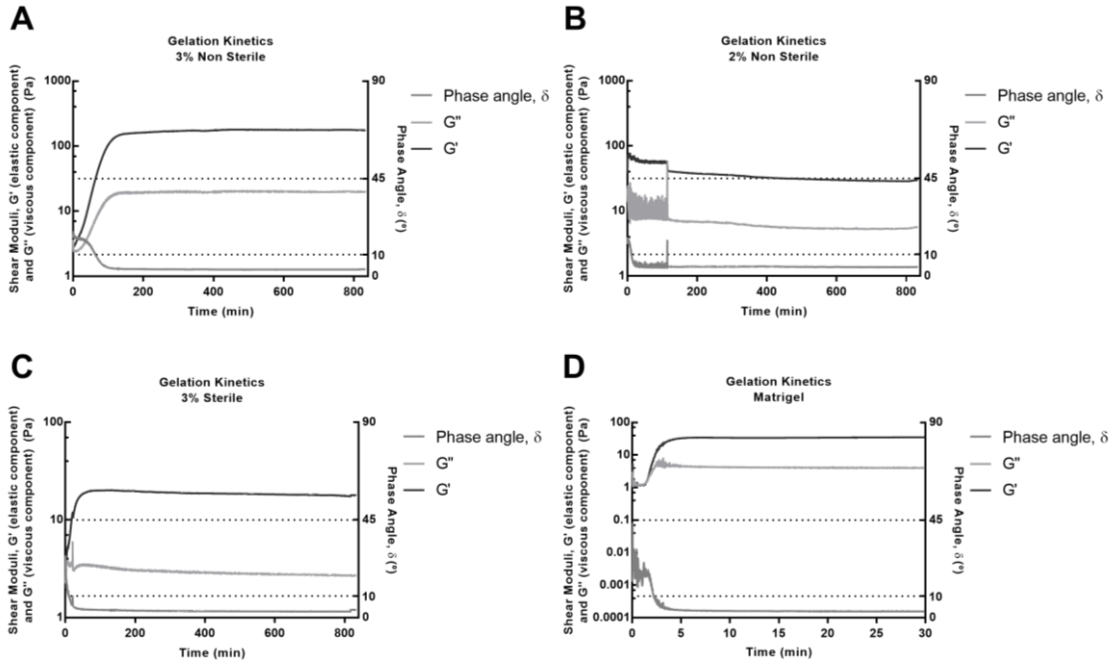

Figure 15 – Rheological properties of dECM – gelation kinetics. A: 3% Non sterile; B: 2% Non sterile; C: 3% sterile; D: Matrigel (n=3).

Matrigel™ exhibited a different behaviour from that of dECM hydrogels, rapidly changing from a viscous-like to a solid-like behaviour as the temperature increased, and attaining stabilization of viscoelastic properties within a few minutes. Also, while pre-gel sterile (3 wt.%) and non-sterile (2 wt.%) dECM samples present G' values in the same range of Matrigel™, the non-sterile dECM at 3 wt.% presented a G' value that was nearly 3x higher than that of Matrigel™. These differences may have major implications for cell culture

Concerning the non-sterile samples tested, results demonstrate that the stiffness of the final hydrogel could be tuned by adjusting the ECM concentration in the pre-gel

solution. This was expected, and similar conclusions have been reported in several studies. [79], [82], [96], [142] On the other hand, when comparing sterile with not-sterile samples at the same concentration (3 wt.%), the former resulted in softer hydrogels. Therefore, although we cannot give any valid explanation for this effect at this time, results suggest that the sterilization process impaired the hydrogel-forming ability of solubilized dECM.

1.9. Cell culture in dECM hydrogel

Fibroblasts and MSC were cultured on-top of pre-formed dECM hydrogel discs (3 wt. %, sterile and non-sterile), pre-equilibrated in culture medium. Fibroblasts were also cultured under 3D conditions (embedded) in dECM hydrogels (3 wt.%, non-sterile). In some assays, both types of cells and culture conditions were tested using Matrigel™ as control hydrogel.

1.9.1. Cell viability and metabolic activity

Metabolic activity of cells cultured on-top of hydrogel discs was measured using resazurin assay at day 1 and 7 (figure 16A/B). Fibroblasts showed an increase from day 1 to day 7, in both type of hydrogels, with better results being obtained with non-sterile samples. The trend observed for the metabolic activity of MSCs in sterile hydrogels was similar to the one observed for fibroblasts, with an increase throughout time. Unexpectedly for the non-sterile hydrogel, there was a significantly decrease in the fluorescence measured at day 7, as compared to day 1. However, as discussed later, these results were not corroborated by the live dead assay.

Live dead assays were performed at day 1, 3 and 7. Fibroblasts cultured on-top presented high viability at all time points (figure 16C), and were able to spread in both types of hydrogels (sterile and non-sterile) from day 1. Cell density increased along the time of culture, and cells became more aligned, but no significant differences were observed between non-sterile and sterile hydrogels. MSCs also remained alive at all time points (figure 16D). At day 1, some cells were already spread, while others still exhibited a more round shape. From day 1 to 3, an increase on cellular density was observed, but no major differences were detected at day 7. Also, there were no significant differences between both hydrogel types. It is important to highlight, however, that this is not a quantitative assay, nor an adequate assay to take valid conclusions in terms of morphology.

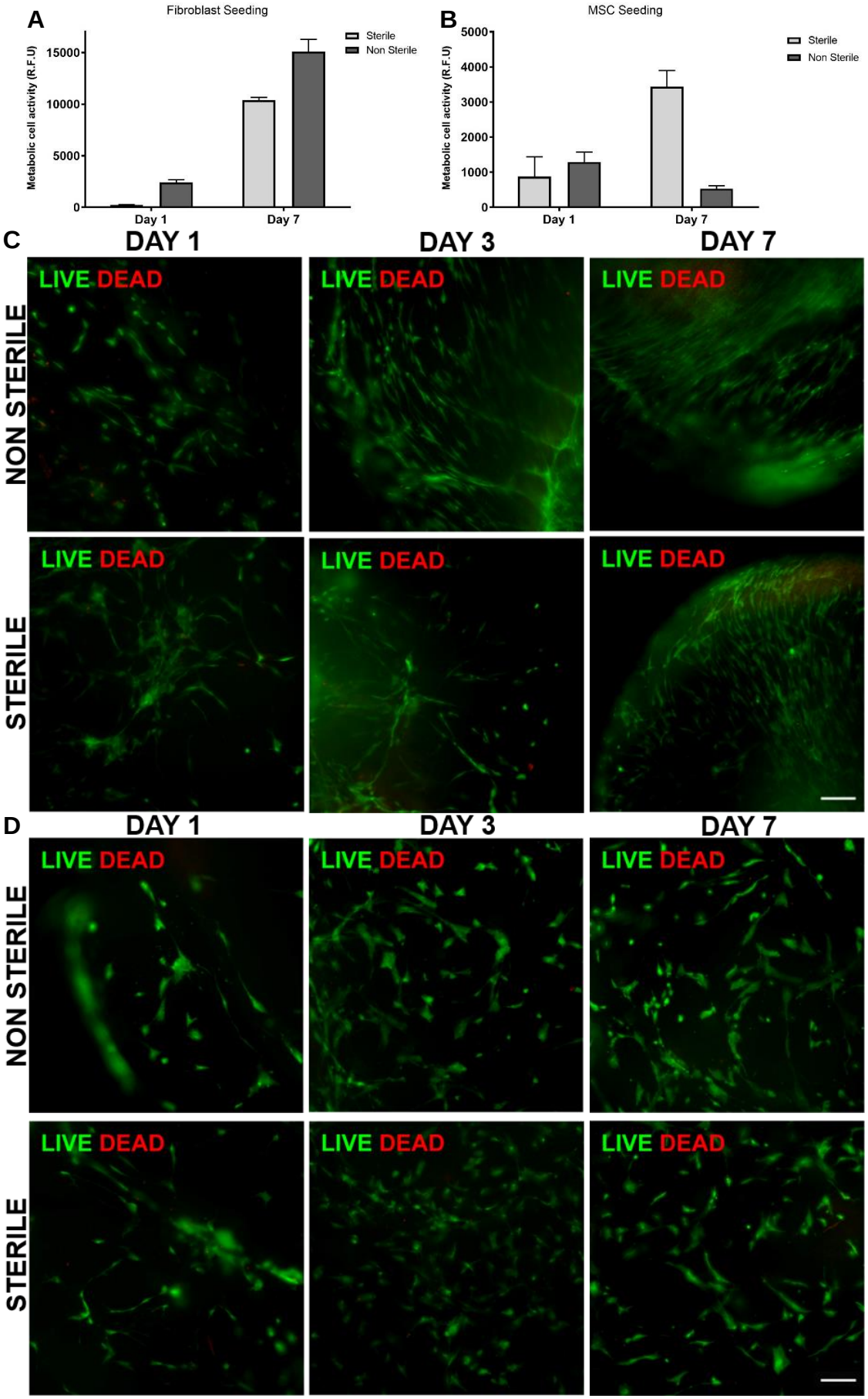

Figure 16 – Metabolic activity and cell viability. A: resazurin assay, fibroblast seeding, day 1 and 7; B: resazurin assay, MSC seeding, day 1 and 7; C: live dead assay, fibroblast seeding, day 1, 3 and 7. Scale bar: 200 µm; D: live dead assay, MSC seeding, day 1, 3 and 7. Scale bar: 200 µm.

For 3D culture, only fibroblasts were embedded in non-sterile hydrogel, but unfortunately at day 1 cells did not showed metabolic activity. Live dead staining revealed that they were mostly dead, while actin staining showed that cells were mostly in a round shape. (Supplementary figure S4). Since the pre-gel solution required some time to form stable hydrogel discs at 37ºC, cells were kept without medium for a rather extensive period of time (3 h were used in this assay). This might explain the high percentage of cells death. In the future, it will be important to improve the properties of the hydrogel (possibly by increasing the dECM concentration) in order to try to reduce the gelling time, as this is a clear requisite for successful cell embedding and posterior 3D culture using these materials.

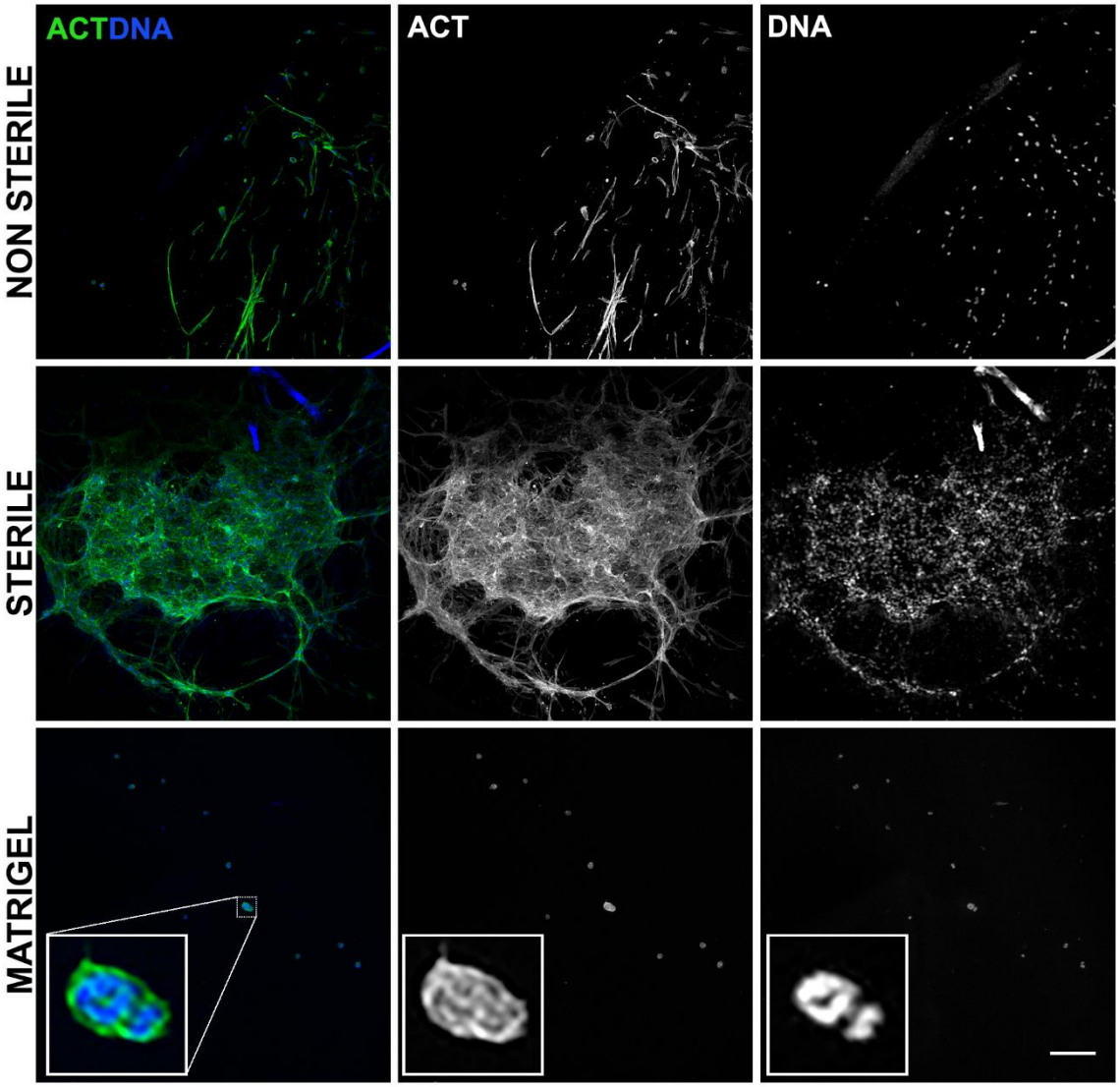

Figure 17 – Morphology of fibroblasts cultured on dECM hydrogel (non sterile, sterile) and on Matrigel™ day 1 with f-actin and DAPI staining. Scale bar: 200 µm

1.9.2. Morphological characterization

Cellular morphology was evaluated through f-actin staining, at day 1, 3 and 7, for both cell types and hydrogel conditions.

At day 1, similar results were obtained for fibroblasts (figure 17) and MSC (figure 18) in both types of hydrogels. Cells were able to spread and acquired a spindle-shape (fibroblasts) or flattened (MSC) morphology on both substrates. A higher cell density was detected in sterile hydrogels, where cell formed dense networks in some regions, as compared to non-sterile hydrogels, where there were fewer adherent cells.

These results are inconsistent with those of the resazurin assay, where both fibroblasts and MSC showed higher metabolic activity on non-sterile hydrogels at day 1, as compared to sterile hydrogels, but we are unable to explain such differences at this stage.

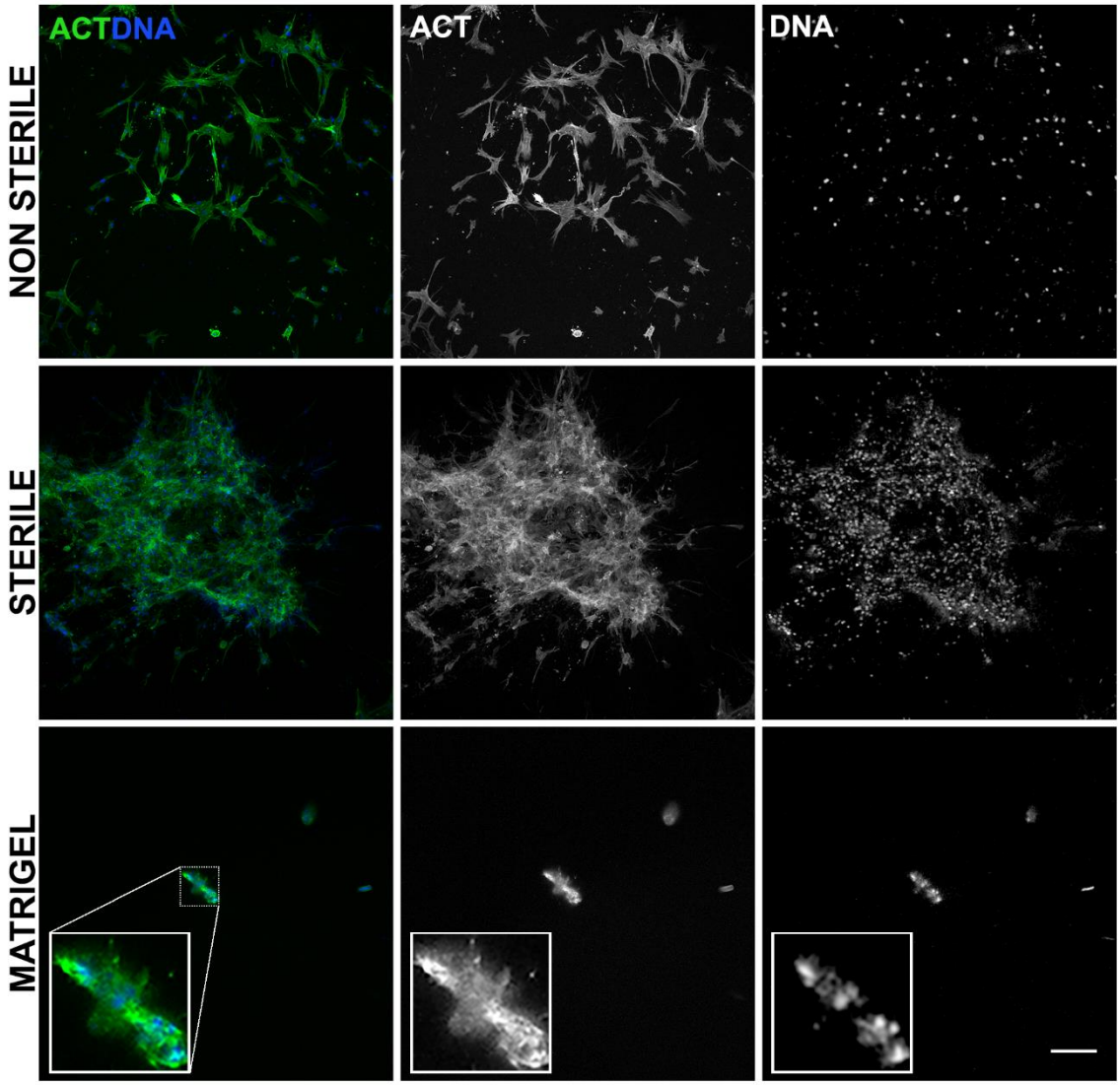

Figure 18 – Morphology of MSCs culture on dECM hydrogel (non sterile, sterile) and on Matrigel™ day 1, with f-actin and DAPI staining. Scale bar: 200 µm.

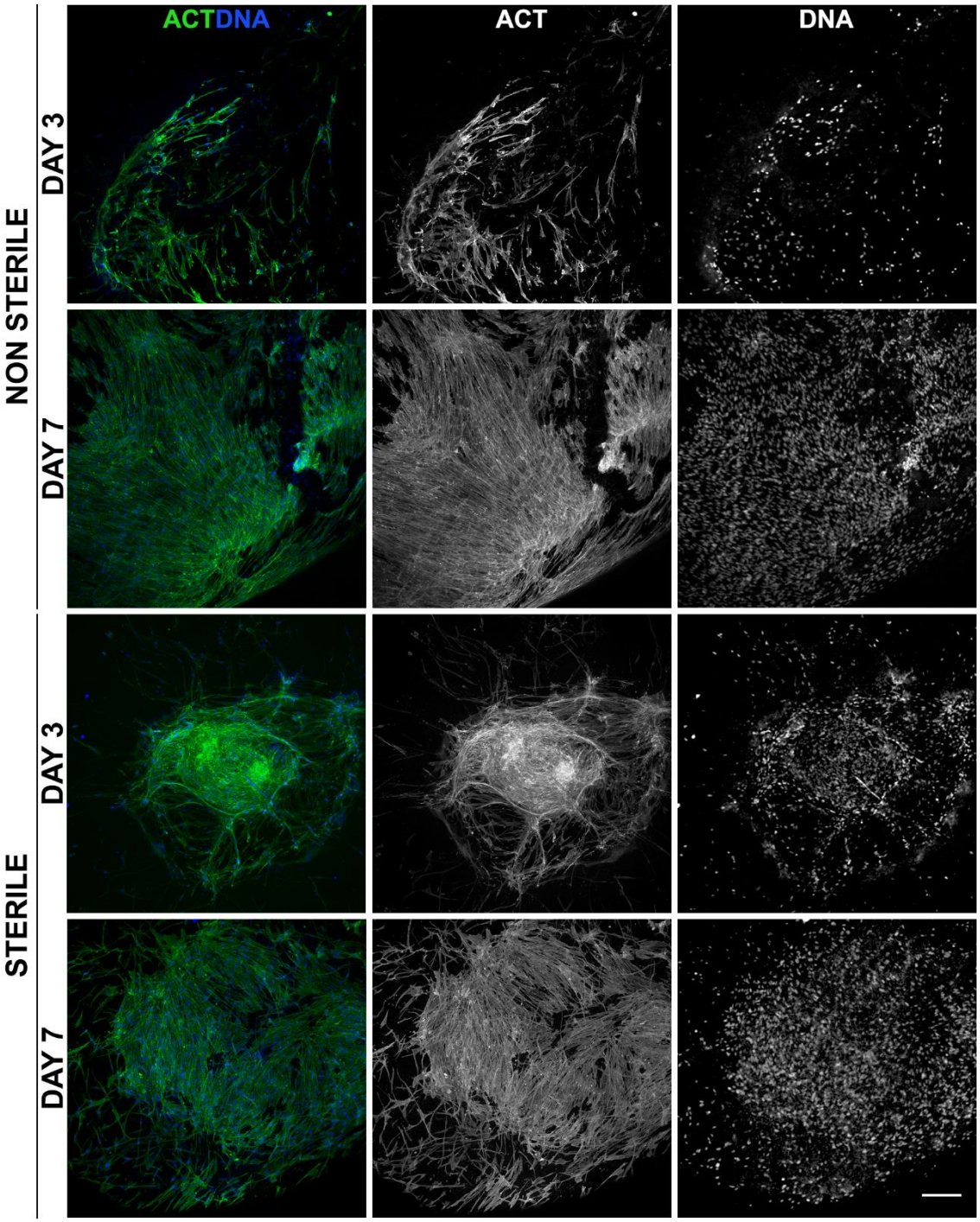

Figure 19 – Fibroblasts morphology at day 3 and 7, in both non sterile and sterile dECM hydrogels, with f-actin and DAPI staining. Scale bar: 200 µm.

Both cell types adhered poorly to Matrigel™, and the few adherent cells did not spread. Some of those cells aggregated, forming small multicellular clusters. It was not possible to obtain results with Matrigel™ discs for the other time points, due to loss of structural integrity, which resulted in difficult handling.

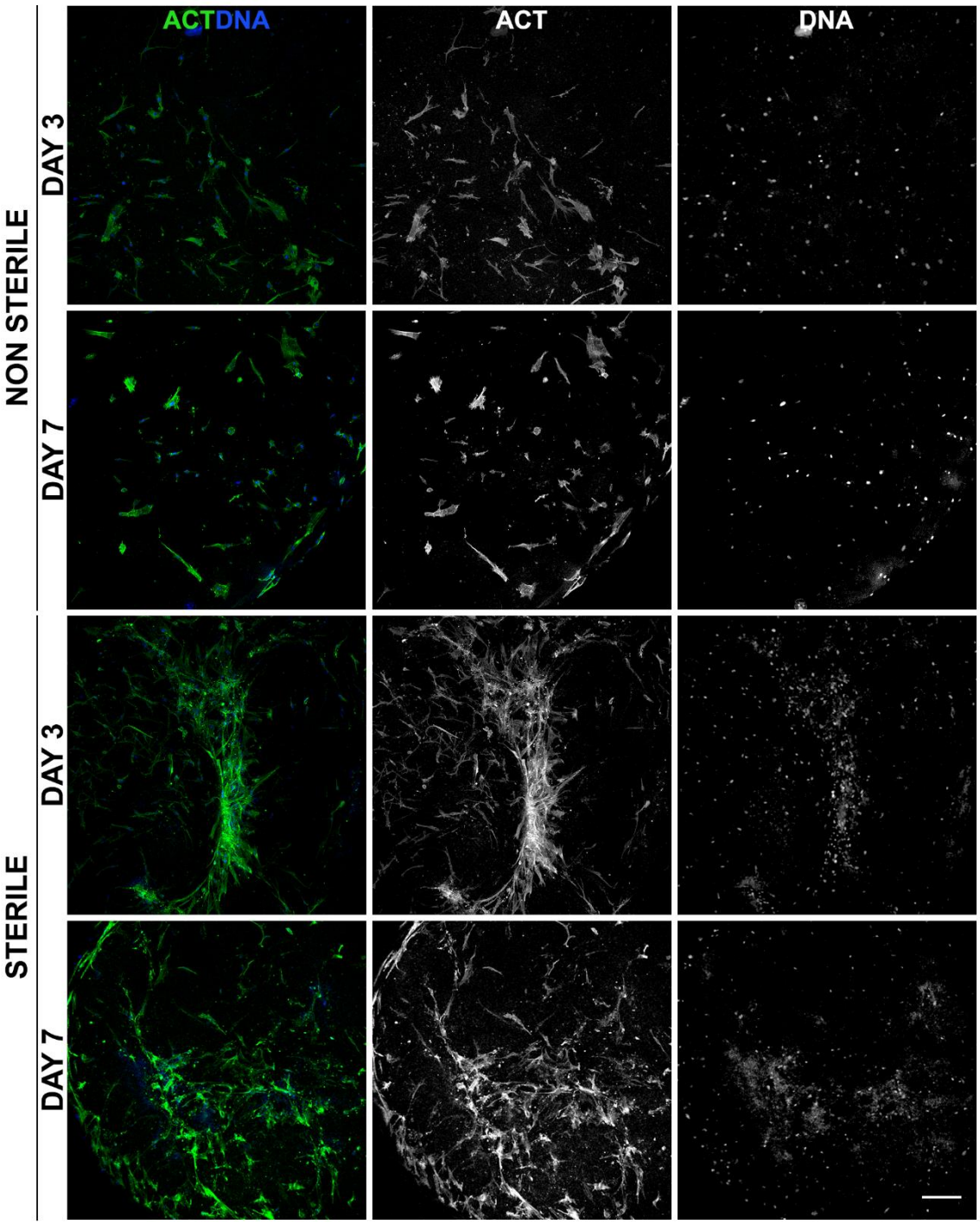

Figure 20 – MSC morphology at day 3 and 7, in both non sterile and sterile hydrogels, with f-actin and DAPI staining. Scale bar: 200 µm.

In accordance to that suggested by the viability assay (figure 16C), fibroblasts were able to proliferate on both hydrogels, with a visible increase on total cell numbers from day 1 (figure 17) to day 3, and from day 3 to day 7 (figure 19). At day 7, a high cell density was observed in the two types of hydrogels, which is in accordance with the

resazurin assay, where fibroblast showed high levels of metabolic activity, in both substrates, and also a significant increase in relation to day 1.

In what concerns MSC culture, fewer cells were detected in non-sterile samples, with no significant differences being observed on cellular density along the time, which is somehow in accordance with the viability and metabolic activity assays.

In sterile hydrogels, the amount of adherent was always higher than that detected on non-sterile hydrogels. Cell density was already at day 1, and differences along the time were more difficult do perceive.

Taking into account results from all time points, fibroblast response to dECM hydrogels showed no significant differences between non-sterile and sterile conditions (figure 19). This suggests that the reported alteration on the hydrogel stiffness and composition did not have a significant effect of fibroblastic cells behaviour. The same was not observed for MSC, where some differences were detected (figure 20). Yet, these results are difficult to interpret, at this stage, since besides differences in their mechanical properties the two types of hydrogels may also differ in their composition. So, any valid conclusions would require a much deeper characterization of sterile vs. non-sterile samples, namely in terms of the presence of growth factors and other bioactive components.

During the assays with both cell types, the size of hydrogel discs considerably decreased along the time of culture, and samples at day 7 were much smaller than at day 1. This may have resulted from cellular activity, which resulted on hydrogel contraction, a phenomenon widely described in the literatures for fibroblasts in floating collagen hydrogels. [149], [150] It may also be associated to some hydrogel degradation of the under culture conditions. Interestingly, although the non-sterile hydrogel samples were not subjected to any sterilization treatment, no contamination was detected along the culture.

Importantly, although the results have shown some inconsistencies that require assays to be repeated in the future for validation, dECM hydrogels appear to provide a microenvironment favourable to cell culture, supporting cell adhesion, viability and proliferation.

Page intentionally left in blank

Conclusions and Future work

Decellularization of placental maternal villous tissue was successfully achieved, with preservation of ECM proteins and GAGs within the tissue. Cellular and nuclear components removal was nearly fully accomplished, as shown by histological analysis and DNA quantification. This validates the proposed decellularization protocol, which represents an optimization from a previously reported protocol, promoting faster and less destructive decellularization.

Sterilization of tissue samples using supercritical fluids, a promising but still largely unexplored technology, was also explored, as successful sterilization dECM is a key requirement for future application of these materials. While the process was efficient in removing pathogens, alterations in the rheological properties of subsequently formed hydrogels, were verified. Sterile hydrogels presented lower stiffness than non sterile ones, which, among other things, might have implications on their performance as matrices for 3D cell culture. In the futures, it will be important to adjust some parameters of the sterilization process, namely decreasing its overall the length. Alterative sterilization techniques could also be tested.

Importantly, using an optimized solubilization process, it was possible to obtain hydrogels from a specific region of the human placenta, maternal villous tissue, which had never been reported. Rheological experiments showed that the formation of stable hydrogels at 37ºC required some time in contrast to Matrigel™, which rapidly solidifies, as the temperature increases from 4ºC to 37ºC. They can be however manipulated at RT, contrary to Matrigel™ which demands strict maintenance of low temperature during handling to avoid triggering premature gelation. Hydrogels at higher dECM concentration presented higher stiffness, as expected, and rheological properties were affected by sterilization as mentioned before. Studies of frequency and amplitude sweep are still needed; to validate the gelation kinetics studies. Future rheological studies should also address the analysis of hydrogel at concentrations higher than the ones tested here. Increasing the concentration of dECM may lead to a decrease in the gelation time, which will be relevant for successfully establishing 3D cell culture with gel-embedded cells. It would also be interesting to monitor the alterations of hydrogel mechanical properties along culture, since cells were able to significantly contract the hydrogel discs.

The biochemical analysis of solubilized dECM showed unexpected results in terms of protein and GAGs content, among different samples. We hypothesised that such

differences might be explained by miscalculations associated with the difficulties in correctly quantifying the amount of dry ECM weight in the different samples, which was used for normalizing the results. Experiments should be redesigned in order to overcome this issue and get more accurate results. We decided to also prepare and test reconstituted dECM (which was lyophilized after solubilization and then reconstituted), because the possibility of having a ready-to-use lyophilized material is appealing for future applications, namely in terms of storage. Unfortunately, reconstituted dECM did not lead to hydrogel formation (data not shown), so further optimizations of the process are still needed.

Cell culture experiments showed that both type of cells, fibroblasts and MSCs, were able to adhere and spread in the hydrogels (sterile and non-sterile), retaining high viability. However, some contradictory results were obtained and experiments need to be repeated to check for consistency. Concerning on-top cell culture, longer period of culture should be evaluated to better understand cell behaviour, namely to analyse if cells have the ability to migrate through the hydrogel or remain only at the surface. Also, it would be interesting to investigate if cells are able to produce endogenous ECM when cultured on these materials. Cell embedding for “true 3D” culture was not successfully achieved, resulting in high percentage of cell death from day 1. Future work should include two different approaches to understand and try to overcome this situation. On one hand, lower incubation time during gel formation should be tested, as maintaining the cells without medium for 3 h was probably too aggressive. On the other hand, gels at high dECM concentration should also be tested, as already discussed.

Overall, all the experiments should be repeated using placentas from larger numbers of donors, to understand how donor variability might influence the obtained results. Ideally, pools of placentas from a number of donors should be used, as this would certainly contribute to reduce variability. This would be an essential step towards standardization, and would constitute an important advantage of these hydrogels as compared to Matrigel™.

References

[1] R. O. Hynes *et al.*, “The extracellular matrix: not just pretty fibrils.,” *Science*, vol. 326, no. 5957, pp. 1216–9, 2009.

[2] C. Frantz, K. M. Stewart, and V. M. Weaver, “The extracellular matrix at a glance,” *J. Cell Sci.*, vol. 123, no. 24, pp. 4195–4200, 2010.

[3] L. T. Saldin, M. C. Cramer, S. S. Velankar, L. J. White, and S. F. Badylak, “Extracellular matrix hydrogels from decellularized tissues: Structure and function,” *Acta Biomaterialia*, vol. 49. pp. 1–15, 2017.

[4] B. Yue, “Biology of the extracellular matrix: An overview,” *Journal of Glaucoma*, vol. 23, no. 8. pp. S20–S23, 2014.

[5] M. Durbeej, “Laminins,” *Cell and Tissue Research*, vol. 339, no. 1. pp. 259–268, 2010.

[6] A. Neve, F. P. Cantatore, N. Maruotti, A. Corrado, and D. Ribatti, “Extracellular Matrix Modulates Angiogenesis in Physiologicaland Pathological Conditions,” *Biomed Res. Int.*, 2014.

[7] M. Ziganshina, S. Pavlovich, N. Bovin, and G. Sukhikh, “Hyaluronic Acid in Vascular and Immune Homeostasis during Normal Pregnancy and Preeclampsia,” *Acta Naturae*, 2016.

[8] F. Groeber, M. Holeiter, M. Hampel, S. Hinderer, and K. Schenke-Layland, “Skin tissue engineering - In vivo and in vitro applications,” *Advanced Drug Delivery Reviews*, vol. 63, no. 4. pp. 352–366, 2011.

[9] U. A. Stock and J. P. Vacanti, “Tissue engineering: current state and prospects.,” *Annu. Rev. Med.*, vol. 52, no. 1, pp. 443–51, 2001.

[10] J. Heino, M. Huhtala, J. Käpylä, and M. S. Johnson, “Evolution of collagen-based adhesion systems,” *International Journal of Biochemistry and Cell Biology*, vol. 41, no. 2. pp. 341–348, 2009.

[11] S. Neves, R. Pereira, M. Araújo, and C. Barrias, “Chapter 4 – Bioengineered peptide-functionalized hydrogels for tissue regeneration and repair,” in *Peptides and proteins as biomaterials for tissue regeneration and repair*, Woodhead Publishing, Elsevier 2018, 2018, pp. 101–125.

[12] S. Hinderer, S. L. Layland, and K. Schenke-Layland, “ECM and ECM-like materials - Biomaterials for applications in regenerative medicine and cancer therapy,” *Advanced Drug Delivery Reviews*, vol. 97. pp. 260–269, 2016.

[13] J. A. Rowley, G. Madlambayan, and D. J. Mooney, “Alginate hydrogels as synthetic extracellular matrix materials,” *Biomaterials*, vol. 20, no. 1, pp. 45–53, 1999.

[14] H. Geckil, F. Xu, X. Zhang, S. Moon, and U. Demirci, “Engineering hydrogels as extracellular matrix mimics,” *Nanomedicine*, vol. 5, no. 3, pp. 469–484, 2010.

[15] N. C. Krejci, C. B. Cuono, R. C. Langdon, and J. McGuire, “In vitro reconstitution of skin: Fibroblasts facilitate keratinocyte growth and differentiation on acellular reticular dermis,” *J. Invest. Dermatol.*, vol. 97, no. 5, pp. 843–848, 1991.

[16] S. F. Badylak *et al.*, “The use of xenogeneic small intestinal submucosa as a biomaterial for Achille’s tendon repair in a dog model,” *J. Biomed. Mater. Res.*, vol. 29, no. 8, pp. 977–985, 1995.

[17] M. F. O’Brien, S. Goldstein, S. Walsh, K. S. Black, R. Elkins, and D. Clarke, “The SynerGraft valve: a new acellular (nonglutaraldehyde-fixed) tissue heart valve for autologous recellularization first experimental studies before clinical implantation.,” *Seminars in thoracic and cardiovascular surgery*, vol. 11, no. 4 Suppl 1. pp. 194–200, 1999.

[18] J. A. Isch, S. A. Engum, C. A. Ruble, M. M. Davis, and J. L. Grosfeld, “Patch esophagoplasty using Alloderm as a tissue scaffold,” in *Journal of Pediatric Surgery*, 2001, vol. 36, no. 2, pp. 266–268.

[19] D. R. Stamov and T. Pompe, “Structure and function of ECM-inspired composite collagen type I scaffolds,” *Soft Matter*, vol. 8, no. 40, p. 10200, 2012.

[20] P. M. Baptista, G. Orlando, S. H. Mirmalek-Sani, M. Siddiqui, A. Atala, and S. Soker, “Whole organ decellularization - A tool for bioscaffold fabrication and organ bioengineering,” in *Proceedings of the 31st Annual International Conference of the IEEE Engineering in Medicine and Biology Society: Engineering the Future of Biomedicine, EMBC 2009*, 2009, pp. 6526–6529.

[21] P. Simon *et al.*, “Early failure of the tissue engineered porcine heart valve SYNERGRAFT™ in pediatric patients,” in *European Journal of Cardio-thoracic Surgery*,

2003, vol. 23, no. 6, pp. 1002–1006.
[22] T. D. Johnson *et al.*, “Quantification of decellularized human myocardial matrix: A comparison of six patients,” *Proteomics - Clinical Applications*, vol. 10, no. 1. pp. 75–83, 2016.
[23] T. W. Gilbert, T. L. Sellaro, and S. F. Badylak, “Decellularization of tissues and organs,” *Biomaterials*, vol. 27, no. 19. pp. 3675–3683, 2006.
[24] T. J. Keane, I. T. Swinehart, and S. F. Badylak, “Methods of tissue decellularization used for preparation of biologic scaffolds and in vivo relevance,” *Methods*, vol. 84. pp. 25–34, 2015.
[25] K. Schenke-Layland *et al.*, “Impact of decellularization of xenogeneic tissue on extracellular matrix integrity for tissue engineering of heart valves,” *J. Struct. Biol.*, vol. 143, no. 3, pp. 201–208, 2003.
[26] P. Lin, W. C. W. Chan, S. F. Badylak, and S. N. Bhatia, “Assessing Porcine Liver-Derived Biomatrix for Hepatic Tissue Engineering,” *Tissue Eng.*, vol. 10, no. 7–8, pp. 1046–1053, 2004.
[27] D. W. Jackson, E. S. Grood, B. T. Cohn, S. P. Arnoczky, T. M. Simon, and J. F. Cummings, “The effects of in situ freezing on the anterior cruciate ligament. An experimental study in goats.,” *J. Bone Joint Surg. Am.*, vol. 73, no. 2, pp. 201–13, 1991.
[28] D. W. Jackson, E. S. Grood, S. P. Arnoczky, D. L. Butler, and T. M. Simon, “Cruciate reconstruction using freeze dried anterior cruciate ligament allograft and a ligament augmentation device LAD:An experimental study in a goat model,” *Am. J. Sports Med.*, vol. 15, no. 6, pp. 528–538, 1987.
[29] K. Sawada, D. Terada, T. Yamaoka, S. Kitamura, and T. Fujisato, “Cell removal with supercritical carbon dioxide for acellular artificial tissue,” *J. Chem. Technol. Biotechnol.*, vol. 83, no. 6, pp. 943–949, 2008.
[30] P. N. Nonaka *et al.*, “Effects of freezing/thawing on the mechanical properties of decellularized lungs,” *J. Biomed. Mater. Res. - Part A*, vol. 102, no. 2, pp. 413–419, 2014.
[31] S. Cebotari *et al.*, “Detergent decellularization of heart valves for tissue engineering: Toxicological effects of residual detergents on human endothelial cells,” *Artif. Organs*, vol. 34, no. 3, pp. 206–210, 2010.
[32] Pulver, A. Shevtsov, B. Leybovich, I. Artyuhov, Y. Maleev, and A. Peregudov, “Production of organ extracellular matrix using a freeze-thaw cycle employing extracellular cryoprotectants,” *Cryo Letters*, vol. 35, no. 5, pp. 400–406, 2014.
[33] S. F. Badylak, “Decellularized allogeneic and xenogeneic tissue as a bioscaffold for regenerative medicine: Factors that influence the host response,” *Ann. Biomed. Eng.*, vol. 42, no. 7, pp. 1517–1527, 2014.
[34] P. M. Crapo, T. W. Gilbert, and S. F. Badylak, “An overview of tissue and whole organ decellularization processes,” *Biomaterials*, vol. 32, no. 12. pp. 3233–3243, 2011.
[35] M. Gonzalez-Andrades, J. de la Cruz Cardona, A. M. Ionescu, A. Campos, M. del Mar Perez, and M. Alamino, “Generation of bioengineered corneas with decellularized xenografts and human keratocytes,” *Investig. Ophthalmol. Vis. Sci.*, vol. 52, no. 1, pp. 215–220, 2011.
[36] I. Prasertsung, S. Kanokpanont, T. Bunaprasert, V. Thanakit, and S. Damrongsakkul, “Development of acellular dermis from porcine skin using periodic pressurized technique,” *J. Biomed. Mater. Res. - Part B Appl. Biomater.*, vol. 85, no. 1, pp. 210–219, 2008.
[37] M. Huang *et al.*, “Using acellular porcine limbal stroma for rabbit limbal stem cell microenvironment reconstruction,” *Biomaterials*, vol. 32, no. 31, pp. 7812–7821, 2011.
[38] D. O. Freytes, S. F. Badylak, T. J. Webster, L. A. Geddes, and A. E. Rundell, “Biaxial strength of multilaminated extracellular matrix scaffolds,” *Biomaterials*, vol. 25, no. 12, pp. 2353–2361, 2004.
[39] J. E. Reing *et al.*, “The effects of processing methods upon mechanical and biologic properties of porcine dermal extracellular matrix scaffolds,” *Biomaterials*, vol. 31, no. 33, pp. 8626–8633, 2010.
[40] X. Dong *et al.*, “RGD-modified acellular bovine pericardium as a bioprosthetic scaffold for tissue engineering,” *J. Mater. Sci. Mater. Med.*, vol. 20, no. 11, pp. 2327–2336, 2009.
[41] A. M. Seddon, P. Curnow, and P. J. Booth, “Membrane proteins, lipids and detergents: Not just a soap opera,” *Biochimica et Biophysica Acta - Biomembranes*, vol. 1666, no. 1–2. pp. 105–117, 2004.

[42] J. S. Cartmell and M. G. Dunn, “Effect of chemical treatments on tendon cellularity and mechanical properties,” *J. Biomed. Mater. Res.*, vol. 49, no. 1, pp. 134–140, 2000.
[43] T. Woods and P. F. Gratzer, “Effectiveness of three extraction techniques in the development of a decellularized bone-anterior cruciate ligament-bone graft,” *Biomaterials*, vol. 26, no. 35, pp. 7339–7349, 2005.
[44] R. W. Grauss, M. G. Hazekamp, F. Oppenhuizen, C. J. Van Munsteren, A. C. Gittenberger-De Groot, and M. C. DeRuiter, “Histological evaluation of decellularised porcine aortic valves: Matrix changes due to different decellularisation methods,” in *European Journal of Cardio-thoracic Surgery*, 2005, vol. 27, no. 4, pp. 566–571.
[45] P. Vavken, S. Joshi, and M. M. Murray, “TRITON-X is most effective among three decellularization agents for ACL tissue engineering,” *J. Orthop. Res.*, vol. 27, no. 12, pp. 1612–1618, 2009.
[46] K. H. Nakayama, C. A. Batchelder, C. I. Lee, and A. F. Tarantal, “Decellularized Rhesus Monkey Kidney as a Three-Dimensional Scaffold for Renal Tissue Engineering,” *Tissue Eng. Part A*, vol. 16, no. 7, pp. 2207–2216, 2010.
[47] B. D. Elder, D. H. Kim, and K. A. Athanasiou, “Developing an articular cartilage decellularization process toward facet joint cartilage replacement,” *Neurosurgery*, vol. 66, no. 4, pp. 722–727, 2010.
[48] R.-N. Chen, H.-O. Ho, Y.-T. Tsai, and M.-T. Sheu, “Process development of an acellular dermal matrix (ADM) for biomedical applications,” *Biomaterials*, vol. 25, no. 13, pp. 2679–2686, 2004.
[49] L. Du, X. Wu, K. Pang, and Y. Yang, “Histological evaluation and biomechanical characterisation of an acellular porcine cornea scaffold,” *Br. J. Ophthalmol.*, vol. 95, no. 3, pp. 410–414, 2011.
[50] S. L. M. Dahl, J. Koh, V. Prabhakar, and L. E. Niklason, “Decellularized native and engineered arterial scaffolds for transplantation,” *Cell Transplant.*, vol. 12, no. 6, pp. 659–666, 2003.
[51] T. W. Hudson, S. Y. Liu, and C. E. Schmidt, “Engineering an improved acellular nerve graft via optimized chemical processing.,” *Tissue Eng.*, vol. 10, no. 9–10, pp. 1346–1358, 2004.
[52] T. W. T. Hudson *et al.*, “Optimized acellular nerve graft is immunologically tolerated and supports regeneration.,” *Tissue Eng.*, vol. 10, no. 11–12, pp. 1641–51, 2004.
[53] T. H. Petersen *et al.*, “Tissue-engineered lungs for in vivo implantation,” *Science (80-.).*, vol. 329, no. 5991, pp. 538–541, 2010.
[54] L. Gui, S. A. Chan, C. K. Breuer, and L. E. Niklason, “Novel Utilization of Serum in Tissue Decellularization,” *Tissue Eng. Part C Methods*, vol. 16, no. 2, pp. 173–184, 2010.
[55] S. B. Lumpkins, N. Pierre, and P. S. McFetridge, “A mechanical evaluation of three decellularization methods in the design of a xenogeneic scaffold for tissue engineering the temporomandibular joint disc,” *Acta Biomater.*, vol. 4, no. 4, pp. 808–816, 2008.
[56] C. R. Deeken *et al.*, “Method of preparing a decellularized porcine tendon using tributyl phosphate,” *J. Biomed. Mater. Res. - Part B Appl. Biomater.*, vol. 96 B, no. 2, pp. 199–206, 2011.
[57] C. C. Xu, R. W. Chan, and N. Tirunagari, “A Biodegradable, Acellular Xenogeneic Scaffold for Regeneration of the Vocal Fold Lamina Propria,” *Tissue Eng.*, vol. 13, no. 3, pp. 551–566, 2007.
[58] M. Srinivasan, D. Sedmak, and S. Jewell, “Effect of fixatives and tissue processing on the content and integrity of nucleic acids,” *American Journal of Pathology*, vol. 161, no. 6. pp. 1961–1971, 2002.
[59] C. V. Montoya and P. S. McFetridge, “Preparation of ex vivo-based biomaterials using convective flow decellularization.,” *Tissue Eng. Part C. Methods*, vol. 15, no. 2, pp. 191–200, 2009.
[60] S. Sasaki *et al.*, “In vivo evaluation of a novel scaffold for artificial corneas prepared by using ultrahigh hydrostatic pressure to decellularize porcine corneas.,” *Mol. Vis.*, vol. 15, no. May, pp. 2022–2028, 2009.
[61] R. J. Levy, N. Vyavahare, M. Ogle, P. Ashworth, R. Bianco, and F. J. Schoen, “Inhibition of cusp and aortic wall calcification in ethanol- and aluminum-treated bioprosthetic heart valves in sheep: background, mechanisms, and synergism.,” *J. Heart Valve Dis.*, vol. 12, no. 2, p. 209–216; discussion 216, 2003.
[62] H. C. Ott *et al.*, “Perfusion-decellularized matrix: Using nature’s platform to engineer a

bioartificial heart," *Nat. Med.*, vol. 14, no. 2, pp. 213–221, 2008.
[63] J. M. Wainwright *et al.*, "Preparation of Cardiac Extracellular Matrix from an Intact Porcine Heart," *Tissue Eng. Part C Methods*, vol. 16, no. 3, pp. 525–532, 2010.
[64] H. C. Ott *et al.*, "Regeneration and orthotopic transplantation of a bioartificial lung," *Nat. Med.*, vol. 16, no. 8, pp. 927–933, 2010.
[65] A. P. Price, K. A. England, A. M. Matson, B. R. Blazar, and A. Panoskaltsis-Mortari, "Development of a Decellularized Lung Bioreactor System for Bioengineering the Lung: The Matrix Reloaded," *Tissue Eng. Part A*, vol. 16, no. 8, pp. 2581–2591, 2010.
[66] J. Cortiella *et al.*, "Influence of Acellular Natural Lung Matrix on Murine Embryonic Stem Cell Differentiation and Tissue Formation," *Tissue Eng. Part A*, vol. 16, no. 8, pp. 2565–2580, 2010.
[67] T. Shupe, M. Williams, A. Brown, B. Willenberg, and B. E. Petersen, "Method for the decellularization of intact rat liver," *Organogenesis*, vol. 6, no. 2, pp. 134–136, 2010.
[68] B. E. Uygun *et al.*, "Organ reengineering through development of a transplantable recellularized liver graft using decellularized liver matrix," *Nat. Med.*, vol. 16, no. 7, pp. 814–820, 2010.
[69] E. A. Ross *et al.*, "Embryonic Stem Cells Proliferate and Differentiate when Seeded into Kidney Scaffolds," *J. Am. Soc. Nephrol.*, vol. 20, no. 11, pp. 2338–2347, 2009.
[70] P. W. Henderson *et al.*, "Development of an acellular bioengineered matrix with a dominant vascular pedicle," *J. Surg. Res.*, vol. 164, no. 1, pp. 1–5, 2010.
[71] S. R. Meyer, B. Chiu, T. A. Churchill, L. Zhu, J. R. T. Lakey, and D. B. Ross, "Comparison of aortic valve allograft decellularization techniques in the rat," *J. Biomed. Mater. Res. - Part A*, vol. 79, no. 2, pp. 254–262, 2006.
[72] I. Tudorache *et al.*, "Tissue engineering of heart valves: biomechanical and morphological properties of decellularized heart valves.," *J. Heart Valve Dis.*, vol. 16, p. 567–573; discussion 574, 2007.
[73] S. Z. Guo, X. J. Ren, B. Wu, and T. Jiang, "Preparation of the acellular scaffold of the spinal cord and the study of biocompatibility," *Spinal Cord*, vol. 48, no. 7, pp. 576–581, 2010.
[74] N.-C. Cheng, B. T. Estes, H. A. Awad, and F. Guilak, "Chondrogenic Differentiation of Adipose-Derived Adult Stem Cells by a Porous Scaffold Derived from Native Articular Cartilage Extracellular Matrix," *Tissue Eng. Part A*, vol. 15, no. 2, pp. 231–241, 2009.
[75] H. Xu *et al.*, "Host response to human acellular dermal matrix transplantation in a primate model of abdominal wall repair.," *Tissue Eng. Part A*, vol. 14, no. 12, pp. 2009–2019, 2008.
[76] M. Ozeki *et al.*, "Evaluation of decellularized esophagus as a scaffold for cultured esophageal epithelial cells," *J. Biomed. Mater. Res. - Part A*, vol. 79, no. 4, pp. 771–778, 2006.
[77] M. He and A. Callanan, "Comparison of Methods for Whole-Organ Decellularization in Tissue Engineering of Bioartificial Organs," *Tissue Eng. Part B Rev.*, vol. 19, no. 3, pp. 194–208, 2013.
[78] P. Akhyari *et al.*, "The Quest for an Optimized Protocol for Whole-Heart Decellularization: A Comparison of Three Popular and a Novel Decellularization Technique and Their Diverse Effects on Crucial Extracellular Matrix Qualities," *Tissue Eng. Part C Methods*, vol. 17, no. 9, pp. 915–926, 2011.
[79] F. Pati *et al.*, "Printing three-dimensional tissue analogues with decellularized extracellular matrix bioink," *Nat. Commun.*, vol. 5, 2014.
[80] L. F. Tapias and H. C. Ott, "Decellularized scaffolds as a platform for bioengineered organs," *Current Opinion in Organ Transplantation*, vol. 19, no. 2. pp. 145–152, 2014.
[81] A. Soto-Gutierrez *et al.*, "A Whole-Organ Regenerative Medicine Approach for Liver Replacement," *Tissue Eng. Part C Methods*, vol. 17, no. 6, pp. 677–686, 2011.
[82] M. J. Sawkins *et al.*, "Hydrogels derived from demineralized and decellularized bone extracellular matrix," *Acta Biomater.*, vol. 9, no. 8, pp. 7865–7873, 2013.
[83] J. Hodde and M. Hiles, "Virus safety of a porcine-derived medical device: Evaluation of a viral inactivation method," *Biotechnol. Bioeng.*, vol. 79, no. 2, pp. 211–216, 2002.
[84] B. Brown, K. Lindberg, J. Reing, D. B. Stolz, and S. F. Badylak, "The Basement Membrane Component of Biologic Scaffolds Derived from Extracellular Matrix," *Tissue Eng.*, vol. 12, no. 3, pp. 519–526, 2006.
[85] J. P. Hodde, S. F. Badylak, a O. Brightman, and S. L. Voytik-Harbin, "Glycosaminoglycan content of small intestinal submucosa: a bioscaffold for tissue

replacement.," *Tissue Eng.*, vol. 2, no. 3, pp. 209–217, 1996.
[86] J. Hodde, R. Record, R. Tullius, and S. Badylak, "Fibronectin peptides mediate HMEC adhesion to porcine-derived extracellular matrix," *Biomaterials*, vol. 23, no. 8, pp. 1841–1848, 2002.
[87] J. P. Hodde, R. D. Record, H. A. Liang, and S. F. Badylak, "Vascular endothelial growth factor in porcine-derived extracellular matrix," *Endothel. J. Endothel. Cell Res.*, vol. 8, no. 1, pp. 11–24, 2001.
[88] O. Gorschewsky, A. Puetz, K. Riechert, A. Klakow, and R. Becker, "Quantitative analysis of biochemical characteristics of bone-patellar tendon-bone allografts.," *Biomed. Mater. Eng.*, vol. 15, pp. 403–411, 2005.
[89] D. J. Rosario, G. C. Reilly, E. Ali Salah, M. Glover, A. J. Bullock, and S. MacNeil, "Decellularization and sterilization of porcine urinary bladder matrix for tissue engineering in the lower urinary tract," *Regen. Med.*, vol. 3, no. 2, pp. 145–156, 2008.
[90] D. W. Jackson, G. E. Windler, and T. M. Simon, "Intraarticular reaction associated with the use of freeze-dried, ethylene oxide-sterilized bone-patella tendon-bone allografts in the reconstruction of the anterior cruciate ligament.," *AM J Sport. Med*, 1990.
[91] M. F. Moreau, Y. Gallois, M. F. Baslé, and D. Chappard, "Gamma irradiation of human bone allografts alters medullary lipids and releases toxic compounds for osteoblast-like cells," *Biomaterials*, vol. 21, no. 4, pp. 369–376, 2000.
[92] W. Q. Sun and P. Leung, "Calorimetric study of extracellular tissue matrix degradation and instability after gamma irradiation," *Acta Biomater.*, vol. 4, no. 4, pp. 817–826, 2008.
[93] Q.-Q. Qiu, P. Leamy, J. Brittingham, J. Pomerleau, N. Kabaria, and J. Connor, "Inactivation of bacterial spores and viruses in biological material using supercritical carbon dioxide with sterilant," *J. Biomed. Mater. Res. Part B Appl. Biomater.*, vol. 91B, no. 2, pp. 572–578, 2009.
[94] J. L. Wehmeyer, S. Natesan, and R. J. Christy, "Development of a Sterile Amniotic Membrane Tissue Graft Using Supercritical Carbon Dioxide," *Tissue Eng. Part C Methods*, vol. 21, no. 7, pp. 649–659, 2015.
[95] J. L. Balestrini *et al.*, "Sterilization of Lung Matrices by Supercritical Carbon Dioxide," *Tissue Eng. Part C Methods*, vol. 22, no. 3, pp. 260–269, 2016.
[96] J. S. Lee *et al.*, "Liver extracellular matrix providing dual functions of two-dimensional substrate coating and three-dimensional injectable hydrogel platform for liver tissue engineering," *Biomacromolecules*, vol. 15, no. 1, pp. 206–218, 2014.
[97] D. O. Freytes, J. Martin, S. S. Velankar, A. S. Lee, and S. F. Badylak, "Preparation and rheological characterization of a gel form of the porcine urinary bladder matrix," *Biomaterials*, vol. 29, no. 11, pp. 1630–1637, 2008.
[98] C. J. Medberry *et al.*, "Hydrogels derived from central nervous system extracellular matrix," *Biomaterials*, vol. 34, no. 4, pp. 1033–1040, 2013.
[99] J. M. Singelyn, J. A. DeQuach, S. B. Seif-Naraghi, R. B. Littlefield, P. J. Schup-Magoffin, and K. L. Christman, "Naturally derived myocardial matrix as an injectable scaffold for cardiac tissue engineering," *Biomaterials*, vol. 30, no. 29, pp. 5409–5416, 2009.
[100] J. Jang *et al.*, "3D printed complex tissue construct using stem cell-laden decellularized extracellular matrix bioinks for cardiac repair," *Biomaterials*, vol. 112, pp. 264–274, 2017.
[101] Z. Kočí *et al.*, "Extracellular Matrix Hydrogel Derived from Human Umbilical Cord as a Scaffold for Neural Tissue Repair and Its Comparison with Extracellular Matrix from Porcine Tissues," *Tissue Eng. Part C Methods*, vol. 23, no. 6, pp. 333–345, 2017.
[102] M. P. Drake, P. F. Davison, S. Bump, and F. O. Schmitt, "Action of Proteolytic Enzymes on Tropocollagen and Insoluble Collagen," *Biochemistry*, vol. 5, no. 1, pp. 301–312, 1966.
[103] E. J. Miller, "Structural Studies on Cartilage Collagen Employing Limited Cleavage and Solubilization with Pepsin," *Biochemistry*, vol. 11, no. 26, pp. 4903–4909, 1972.
[104] D. J. S. Hulmes, "Collagen diversity, synthesis and assembly," in *Collagen: Structure and Mechanics*, 2008, pp. 15–47.
[105] S. L. Voytik-Harbin, a O. Brightman, B. Z. Waisner, J. P. Robinson, C. H. Lamar, and Anonymous, "Small intestinal submucosa: A tissue-derived extracellular matrix that promotes tissue-specific growth and differentiation of cells in vitro," *Tissue Eng.*, vol. 4, no. 2, pp. 157–174, 1998.
[106] Z. Bohak, "Purification and characterization of chicken pepsinogen and chicken pepsin.," *J. Biol. Chem.*, vol. 244, no. 17, pp. 4638–4648, 1969.
[107] W. E. Hornbuckle, K. W. Simpson, and B. C. Tennant, "Gastrointestinal Function," in

Clinical Biochemistry of Domestic Animals, 2008, pp. 413–457.
[108] A. Bougatef and R. Balti, “Food Chemistry Pepsinogen and pepsin from the stomach of smooth hound (Mustelus mustelus): Purification , characterization and amino acid terminal sequences,” vol. 107, pp. 777–784, 2008.
[109] C. S. Hughes, L. M. Postovit, and G. A. Lajoie, “Matrigel: a complex protein mixture required for optimal growth of cell culture.,” *Proteomics*, vol. 10, no. 9, pp. 1886–1890, 2010.
[110] Y. Fang and R. M. Eglen, “Three-Dimensional Cell Cultures in Drug Discovery and Development,” *SLAS Discovery*, vol. 22, no. 5. pp. 456–472, 2017.
[111] S. Uriel *et al.*, “The role of adipose protein derived hydrogels in adipogenesis,” *Biomaterials*, vol. 29, no. 27, pp. 3712–3719, 2008.
[112] H. Gray, *Anatomy of the human body*. 1918.
[113] R. Sood, J. L. Zehnder, M. L. Druzin, and P. O. Brown, “Gene expression patterns in human placenta.,” *Proc. Natl. Acad. Sci. U. S. A.*, vol. 103, no. 14, pp. 5478–83, 2006.
[114] E. James, G. Meschia, and F. Battaglia, “A-V differences of free fatty acids and glycerol in the ovine umbilical circulation.,” *Proc Soc Exp Biol Med*, vol. 138, pp. 823–6, 1971.
[115] M. I. Zakowski and N. L. Herman, “The Placenta: Anatomy, Physiology, and Transfer of Drugs,” *Chestnut’s Obstet. Anesth.*, pp. 55–72, 2004.
[116] B. Huppertz, “The anatomy of the normal placenta,” *Journal of Clinical Pathology*, vol. 61, no. 12. pp. 1296–1302, 2008.
[117] G. M. Bouw, L. A. M. Stolte, J. P. A. Baak, and J. Oort, “Quantitative morphology of the placenta 1. Standardization of sampling,” *Eur. J. Obstet. Gynecol. Reprod. Biol.*, vol. 6, no. 6, pp. 325–331, 1976.
[118] M. R. Davidson, M. L. London, and P. W. Ladewig, *Olds’ maternal-newborn nursing & women’s health across the lifespan*, 6th ed. 2012.
[119] R. Leiser, G. Kosanke, and P. Kaufmann, “Human placental vascularization: Structural and quantitative aspects,” in *Placenta: Basic Research for Clinical Application*, Basel, Switzerland: Karger, 1991, pp. 32–45.
[120] J. Boyd and W. Hamilton, *The human placenta.* 1970.
[121] A. E. Wallace, R. Fraser, and J. E. Cartwright, “Extravillous trophoblast and decidual natural killer cells: A remodelling partnership,” *Human Reproduction Update*, vol. 18, no. 4. pp. 458–471, 2012.
[122] K. Benirschke and P. Kaufmann, *Pathology of the Human Placenta*, vol. 82, no. 9. 2000.
[123] L. Arey, *Developmental Anatomy: A Textbook and Laboratory Manual of Embryology*. 1974.
[124] C. P. Chen and J. D. Aplin, “Placental extracellular matrix: Gene expression, deposition by placental fibroblasts and the effect of oxygen,” *Placenta*, vol. 24, no. 4, pp. 316–325, 2003.
[125] P. S. Amenta, S. Gay, A. Vaheri, and A. Martinez-Hernandez, “The extracellular matrix is an integrated unit: ultrastructural localization of collagen types I, III, IV, V, VI, fibronectin, and laminin in human term placenta.,” *Coll. Relat. Res.*, vol. 6, no. 2, pp. 125–52, 1986.
[126] T. Yamada, M. Isemura, Y. Yamaguchi, H. Munakata, N. Hayashi, and M. Kyogoku, “Immunohistochemical localization of fibronectin in the human placentas at their different stages of maturation,” *Histochemistry*, vol. 86, no. 6, pp. 579–584, 1987.
[127] H. J. Church, A. J. Richards, and J. D. Aplin, “Laminins in decidua, placenta and choriocarcinoma cells,” *Placenta*, vol. 18, pp. 143–162, 1997.
[128] M. Korhonen and I. Virtanen, “Immunohistochemical localization of laminin and fibronectin isoforms in human placental villi,” *J. Histochem. Cytochem.*, vol. 49, no. 3, pp. 313–322, 2001.
[129] B. B. Arbeille, F. M. J. Fauvel-Lafeve, M. B. Lemesle, D. Tenza, and Y. J. Legrand, “Thrombospondin: A component of microfibrils in various tissues,” *J. Histochem. Cytochem.*, vol. 39, no. 10, pp. 1367–1375, 1991.
[130] M. Castellucci, I. Classen-Linke, J. M??hlhauser, P. Kaufmann, L. Zardi, and R. Chiquet-Ehrismann, “The human placenta: a model for tenascin expression,” *Histochemistry*, vol. 95, no. 5, pp. 449–458, 1991.
[131] B. F. King and T. N. Blankenship, “Immunohistochemical localization of fibrillin in developing macaque and term human placentas and fetal membranes,” *Microsc. Res. Tech.*, vol. 38, no. 1–2, pp. 42–51, 1997.
[132] J. S. Choi, J. D. Kim, H. S. Yoon, and Y. W. Cho, “Full-Thickness Skin Wound Healing Using Human Placenta-Derived Extracellular Matrix Containing Bioactive Molecules,” .

[133] M. Gholipourmalekabadi *et al.*, “Decellularized human amniotic membrane: More is needed for an efficient dressing for protection of burns against antibiotic-resistant bacteria isolated from burn patients,” *Burns*, vol. 41, no. 7, pp. 1488–1497, 2015.
[134] R. Roy *et al.*, “Decellularized amniotic membrane attenuates postinfarct left ventricular remodeling,” *J. Surg. Res.*, vol. 200, no. 2, pp. 409–419, 2016.
[135] M. P. Francis *et al.*, “Human placenta hydrogel reduces scarring in a rat model of cardiac ischemia and enhances cardiomyocyte and stem cell cultures,” *Acta Biomater.*, vol. 52, pp. 92–104, 2017.
[136] K. H. Schneider *et al.*, “Decellularized human placenta chorion matrix as a favorable source of small-diameter vascular grafts,” *Acta Biomater.*, vol. 29, pp. 125–134, 2016.
[137] J. P. Bennett, R. Matthews, and W. P. Faulk, “TREATMENT OF CHRONIC ULCERATION OF THE LEGS WITH HUMAN AMNION,” *Lancet*, vol. 315, no. 8179, pp. 1153–1156, 1980.
[138] B. Bose, “Burn wound dressing with human amniotic membrane,” *Ann. R. Coll. Surg. Engl.*, vol. 61, no. 6, pp. 444–447, 1979.
[139] H. S. Dua, J. A. P. Gomes, A. J. King, and V. S. Maharajan, “The amniotic membrane in ophthalmology,” *Survey of Ophthalmology*, vol. 49, no. 1. pp. 51–77, 2004.
[140] C. Lee *et al.*, “Bioinspired, calcium-free alginate hydrogels with tunable physical and mechanical properties and improved biocompatibility,” *Biomacromolecules*, vol. 14, no. 6, pp. 2004–2013, 2013.
[141] C. Bibbo, S. E. Little, J. Bsat, K. A. Botka, C. Benson, and J. N. Robinson, “Chorioamniotic Separation Found on Obstetric Ultrasound and Perinatal Outcome,” *Am. J. Perinatol.*, 2016.
[142] M. W. Tibbitt and K. S. Anseth, “Hydrogels as extracellular matrix mimics for 3D cell culture,” *Biotechnology and Bioengineering*, vol. 103, no. 4. pp. 655–663, 2009.
[143] N. Shirakigawa, H. Ijima, and T. Takei, “Decellularized liver as a practical scaffold with a vascular network template for liver tissue engineering,” *J. Biosci. Bioeng.*, vol. 114, no. 5, pp. 546–551, 2012.
[144] D. C. Sullivan *et al.*, “Decellularization methods of porcine kidneys for whole organ engineering using a high-throughput system,” *Biomaterials*, vol. 33, no. 31, pp. 7756–7764, 2012.
[145] A. C. Gonçalves, L. G. Griffiths, R. V Anthony, and E. C. Orton, “Decellularization of bovine pericardium for tissue-engineering by targeted removal of xenoantigens.,” *J. Heart Valve Dis.*, pp. 212–217, 2005.
[146] E. Rieder *et al.*, “Decellularization protocols of porcine heart valves differ importantly in efficiency of cell removal and susceptibility of the matrix to recellularization with human vascular cells,” *J. Thorac. Cardiovasc. Surg.*, vol. 127, no. 2, pp. 399–405, 2004.
[147] M. T. Kasimir *et al.*, “The decellularized porcine heart valve matrix in tissue engineering: Platelet adhesion and activation,” *Thromb. Haemost.*, vol. 94, no. 3, pp. 562–567, 2005.
[148] J. M. Zuidema, C. J. Rivet, R. J. Gilbert, and F. A. Morrison, “A protocol for rheological characterization of hydrogels for tissue engineering strategies,” *J. Biomed. Mater. Res. - Part B Appl. Biomater.*, vol. 102, no. 5, pp. 1063–1073, 2014.
[149] Y. K. Zhu *et al.*, “Contraction of fibroblast-containing collagen gels: initial collagen concentration regulates the degree of contraction and cell survival,” *Vitr. Cell. Dev. Biol.*, vol. 37, pp. 10–16, 2001.
[150] M. E. Smithmyer, L. a. Sawicki, and A. M. Kloxin, “Hydrogel scaffolds as in vitro models to study fibroblast activation in wound healing and disease,” *Biomater. Sci.*, vol. 2, no. 5, p. 634, 2014.

Page intentionally left in blank

Supplementary Data

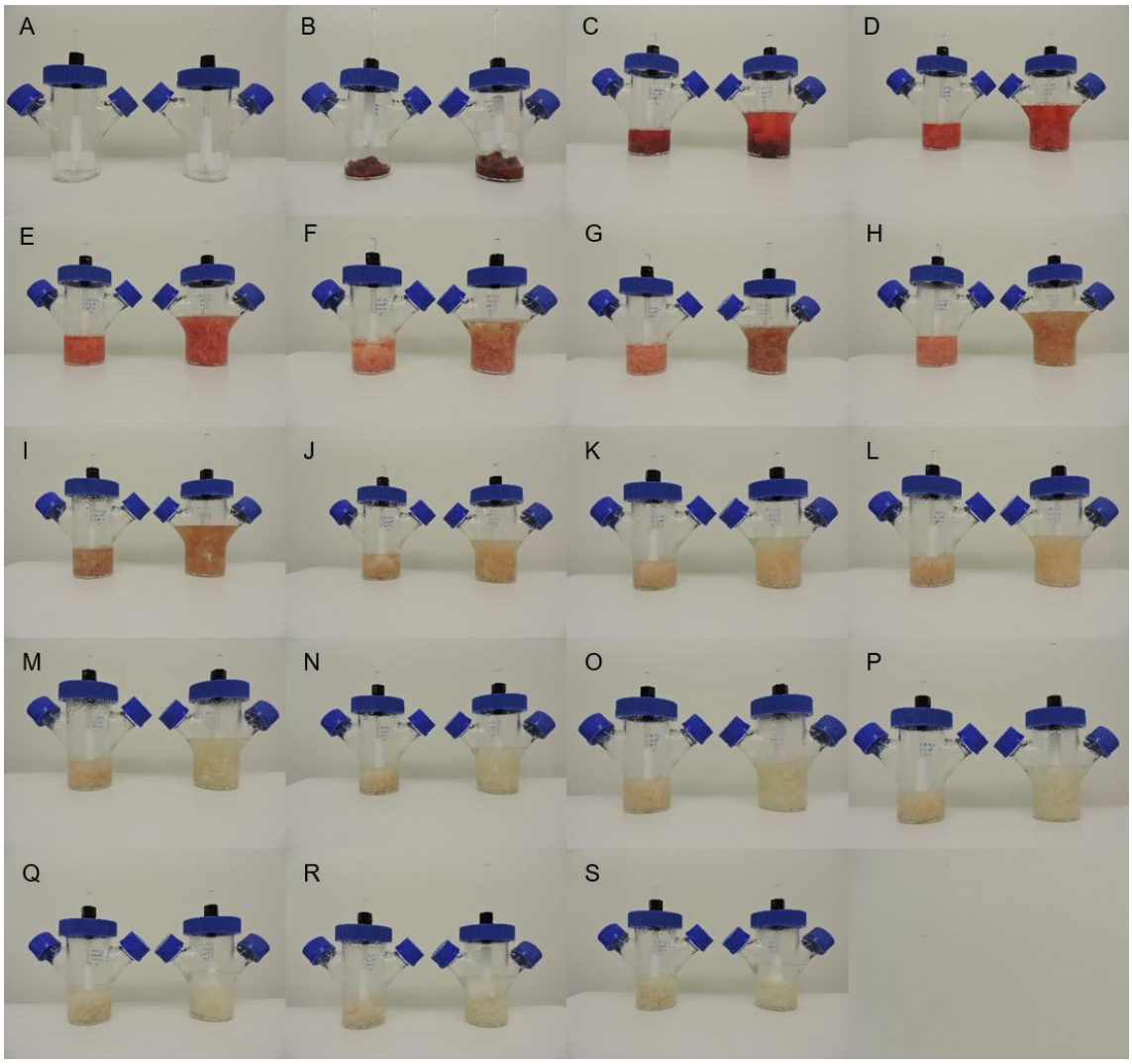

Figure S1 – Full decellularization protocol. A) Spinner flasks; B) day 1 before immersion; C) day 1 before agitaton; D) day 1 after water wash; E) day 1 after water wash F) day 1 before SDS; G) day 1, after SDS; H) day 1, end of the day; I) day 2, after overnight wash; J) day 2, water wash; K) eay 2, water wash; L)day 2, end of the day; M) day 3 after overnight wash; N) day 3 after water wash; O) day 3 after wash; P) day 3 beggining of DNAse treatment; Q) day 4 after DNAse treatment; R) day 4, end of the day; S) day 5, end of the day.

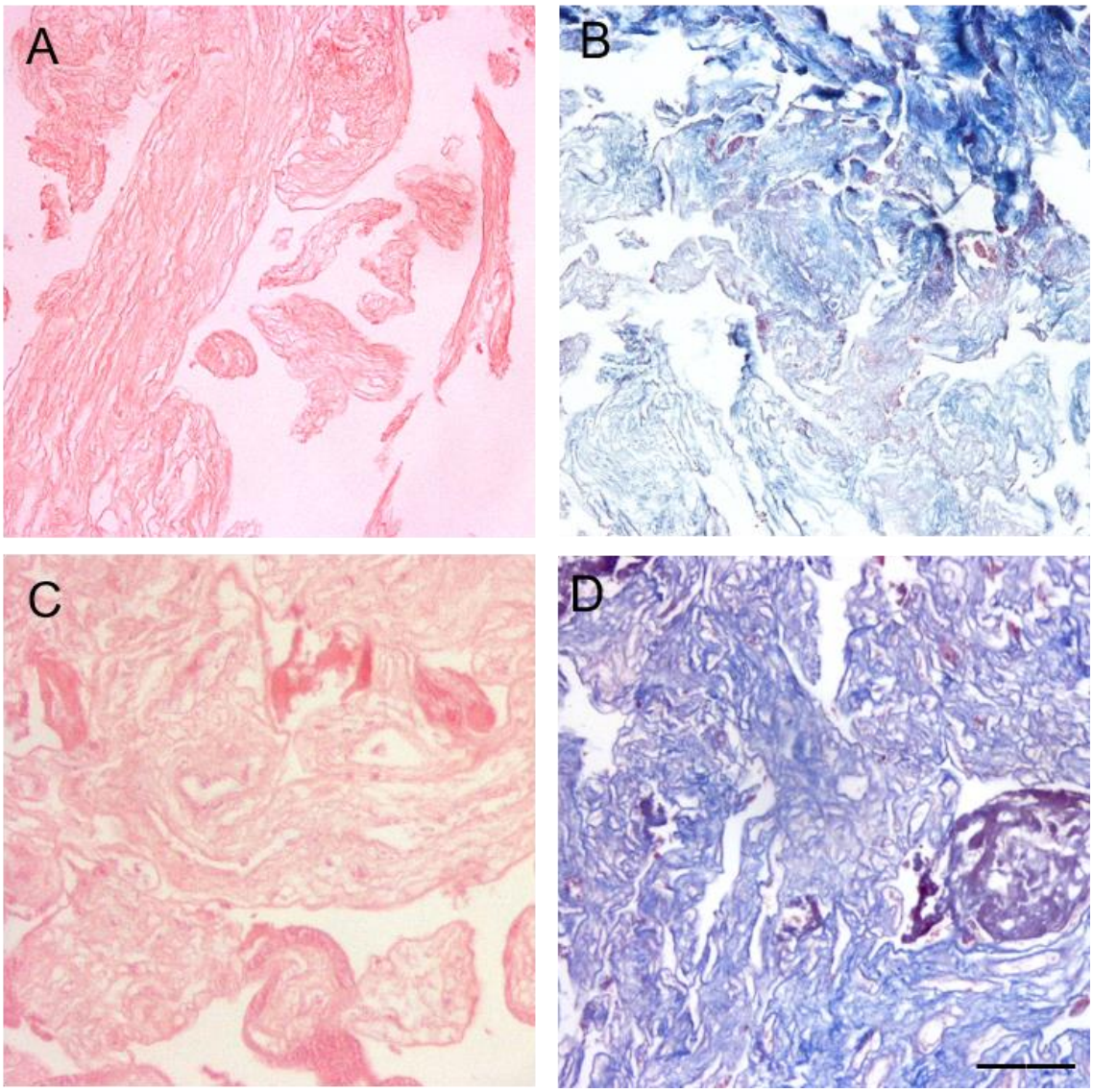

Figure S2 – Protocol validation. A: H&E staining of 8-day protocol decellularized sample; B: TM staining of 8-day protocol decellularized sample; C: H&E staining of 5-day protocol decellularized sample; D: TM staining of 8-day 5-day protocol decellularized sample. Scale bar: 100 µm.

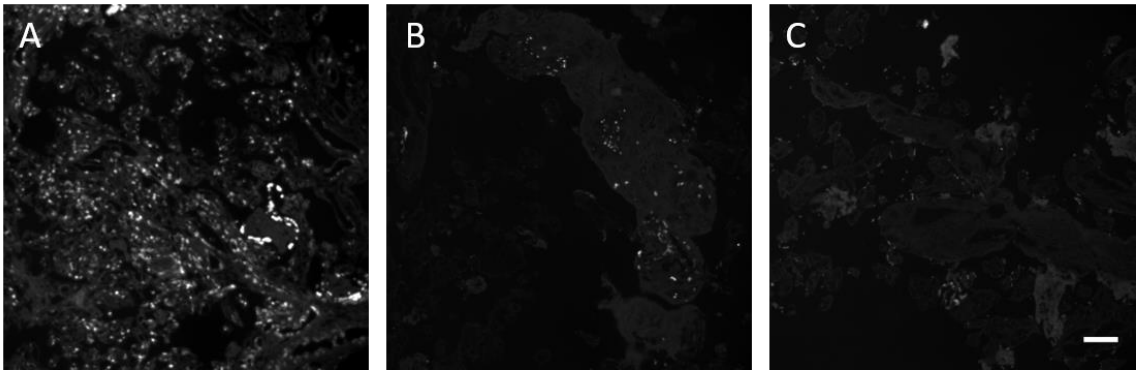

Figure S3 – DNAse treatment evaluation, with DAPI staining. A: 0 h treatment; B: 1 h treatment; C: 3 h treatment. Scale bar: 50 µm

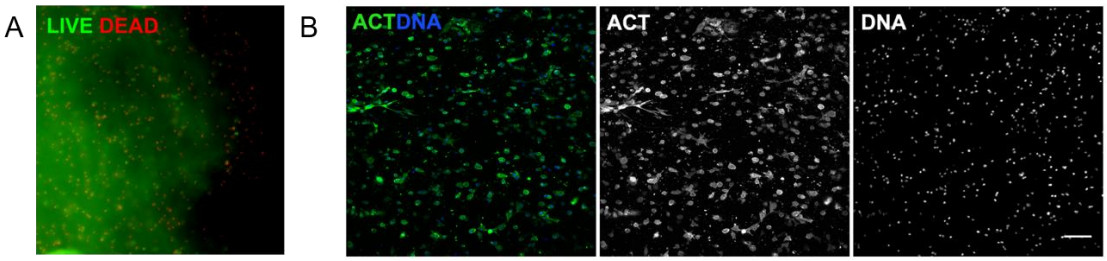

Figure S4 – Fibroblast embedding on 3% non-sterile dECM hydrogel: A – Live Dead staining; B – Actin and DAPI staining. Scale bar: 1000 µm

Page intentionally left in blank